Kaunas University of Technology

Faculty of Mathematics and Natural Sciences

Evaluation of the Absorbed Dose in Blood Samples Using the Dicentric Chromosome Assay

Master's Final Degree Project

Lijana Lileikytė

Project author

Prof. dr. Diana Adlienė

Supervisor

dr. Olga Sevriukova

Consultant

Kaunas, 2022

Kaunas University of Technology

Faculty of Mathematics and Natural Sciences

Evaluation of the Absorbed Dose in Blood Samples Using the Dicentric Chromosome Assay

Master's Final Degree Project

Medical Physics (6213GX001)

Lijana Lileikytė

Project author

Prof. dr. Diana Adlienė

Supervisor

dr. Olga Sevriukova

Consultant

Assoc. Prof. dr. Linas Puodžiukynas

Reviewer

Kaunas, 2022

Kaunas University of Technology

Faculty of Mathematics and Natural Sciences

Lijana Lileikytė

Evaluation of the Absorbed Dose in Blood Samples Using the Dicentric Chromosome Assay

Declaration of Academic Integrity

I confirm the following:

1. I have prepared the final degree project independently and honestly without any violations of the copyrights or other rights of others, following the provisions of the Law on Copyrights and Related Rights of the Republic of Lithuania, the Regulations on the Management and Transfer of Intellectual Property of Kaunas University of Technology (hereinafter – University) and the ethical requirements stipulated by the Code of Academic Ethics of the University;

2. All the data and research results provided in the final degree project are correct and obtained legally; none of the parts of this project are plagiarised from any printed or electronic sources; all the quotations and references provided in the text of the final degree project are indicated in the list of references;

3. I have not paid anyone any monetary funds for the final degree project or the parts thereof unless required by the law;

4. I understand that in the case of any discovery of the fact of dishonesty or violation of any rights of others, the academic penalties will be imposed on me under the procedure applied at the University; I will be expelled from the University and my final degree project can be submitted to the Office of the Ombudsperson for Academic Ethics and Procedures in the examination of a possible violation of academic ethics.

Lijana Lileikytė

Confirmed electronically

Lileikytė, Lijana. Evaluation of the Absorbed Dose in Blood Samples Using the Dicentric Chromosome Assay. Master's Final Degree Project / prof. dr. Diana Adlienė; Faculty of Mathematics and Natural Sciences, Kaunas University of Technology.

Study field and area (study field group): Medical technologies, Health sciences.

Keywords: cytogenetic analysis, biological dosimetry, Dicentric Chromosome Assay, individual radiosensitivity.

Kaunas, 2022. 61 p.

Summary

Cytogenetic analysis can be used to determine both the absorbed dose and the individual radiosensitivity. Sensitivity to ionizing radiation can be an important indicator in providing protection against unjustified exposure and in predicting side effects that occur after radiotherapy treatment or a radiological accident. Cytogenetic analysis for the comparison of evaluated doses using Dicentric Chromosome Assay for the prostate cancer patients has been performed with the aim to identify the difference between Dicentric Chromosome Assay results depending on estimated individual radiosensitivity by using the G2-assay.

Six prostate cancer patients who received a total dose of 62–74 Gy were investigated. The blood samples – prior radiotherapy treatment (2 Gy in vitro) and after completing radiotherapy treatment (in vivo) – were analyzed by the Dicentric Chromosome Assay and using G2-assay. Axio Imager Z2 microscope with a Metasystems Metafer slide analysis system was used for analysis. Dose evaluation was performed using the dose calibration curve provided in the IAEA publication. Biodose Tool software was also used. Permission of Lithuanian Bioethics committee (No. L-14-07/1) was granted for the conduction of this study.

Comparison of estimated and preplanned dose of 2 Gy has shown modest overestimation (2.082–2.528 Gy). The mean estimated dose (2.326 Gy) was significantly higher than 2 Gy (p-value 0.005). Estimated whole-body doses after treatment were from the range of 2.041–2.763 Gy. Estimated Papworth's u-value range was 6.017–17.926, which indicated partial body exposure. The relationship between estimated whole-body doses and total doses delivered to patients during radiotherapy treatment was controversial, thus indicating that the results could be interpreted for each patient individually, since they could be affected by individual radiosensitivity.

In general, clear correlation between estimated doses and individual radiosensitivity before and after radiotherapy treatment was not found, however some tendency of increased radiosensitivity after radiotherapy treatment was observed. Performed investigation has indicated that individual radiosensitivity can affect the results of Dicentric Chromosome Assay. The combination of these assays before radiotherapy treatment can help to predict individual radiosensitivity changes during the radiotherapy course. However, further investigations are needed.

Lileikytė, Lijana. Sugertosios dozės vertinimas kraujo bandiniuose naudojant dicentrinių chromosomų tyrimo metodą. Magistro studijų baigiamasis projektas / vadovė prof. dr. Diana Adlienė; Kauno technologijos universitetas, Matematikos ir gamtos mokslų fakultetas.

Studijų kryptis ir sritis (studijų krypčių grupė): Medicinos technologijos, Sveikatos mokslai.

Reikšminiai žodžiai: citogenetinė analizė, biologinė dozimetrija, dicentrinių chromosomų tyrimas, individualus radiojautrumas.

Kaunas, 2022. 61 p.

Santrauka

Citogenetine analize galima nustatyti ir paciento sugertąją dozę, ir individualų radiojautrumą. Jautrumas jonizuojančiai spinduliuotei gali būti svarbus rodiklis, užtikrinantis apsaugą nuo nepagrįstos apšvitos ir numatant šalutinį poveikį, atsirandantį po radioterapijos gydymo ar radiologinės avarijos. Šio tyrimo metu prostatos vėžiu sergantiems pacientams buvo atlikta citogenetinė analizė, skirta palyginti dicentrinių chromosomų tyrimu įvertintas dozes, siekiant nustatyti ar dicentrinių chromosomų tyrimo rezultatai skirsis priklausomai nuo įvertinto individualaus radiojautrumo naudojant G2 tyrimą.

Buvo tiriami šeši prostatos vėžiu sergantys pacientai, kuriems radioterapijos procedūrų metu suvesta dozė buvo 62–74 Gy. Kraujo mėginiai – prieš radioterapijos kursą (2 Gy in vitro) ir baigus kursą (in vivo) – buvo analizuojami naudojant dicentrinių chromosomų ir G2 tyrimų metodus. Analizei buvo naudojamas mikroskopas Axio Imager Z2 su Metasystems Metafer stiklelių analizės sistema. Dozės įvertinimas buvo atliktas naudojant dozės kalibravimo kreivę, pateiktą TATENA rekomendacijose, ir Biodose Tool programinę įrangą. Šiam tyrimui atlikti buvo gautas Lietuvos bioetikos komiteto leidimas (Nr. L-14-07/1).

Palyginus įvertintas dozes ir suteiktą 2 Gy dozę, buvo nustatytas nedidelis pervertinimas (2,082–2,528 Gy). Įvertintų dozių vidurkis (2,326 Gy) buvo reikšmingai didesnis nei 2 Gy (p vertė 0,005). Tačiau toks pervertinimas yra priimtinas, nes pagal rekomendacijas biologinėje dozimetrijoje leidžiami dozės nuokrypiai yra iki 0,5 Gy. Įvertintos viso kūno dozės po gydymo buvo 2,041–2,763 Gy. Apskaičiuotas u-verčių diapazonas 6,017–17,926 rodo dalinę kūno apšvitą. Ryšys tarp įvertintų viso kūno dozių ir bendrų, radioterapijos metu suteiktų, apšvitos dozių buvo prieštaringas, tai rodo, kad rezultatus galima interpretuoti kiekvienam pacientui atskirai, nes juos gali paveikti individualus radiojautrumas.

Apskritai, aiškios koreliacijos tarp įvertintų dozių ir individualaus radiojautrumo prieš ir po radioterapijos kurso nenustatyta, tačiau pastebėta tam tikra padidėjusio jautrumo jonizuojančiajai spinduliuotei tendencija po radioterapijos kurso. Atliktas tyrimas parodė, kad individualus radiojautrumas gali turėti įtakos dicentrinių chromosomų tyrimo rezultatams. Šių tyrimų derinys prieš radioterapijos kursą gali padėti numatyti individualius radiojautrumo pokyčius. Tačiau tam yra reikalingi tolesni tyrimai.

Table of Contents

List of Figures

List of Tables

Introduction

Ionizing radiation is used to diagnose (X-ray and nuclear medicine diagnostic procedures) and to treat (radiation and nuclear medicine therapy procedures) various diseases. The goal of radiation therapy is to destroy the tumor while protecting the surrounding organs. In other words, give a sufficiently high dose to the tumor and minimal to the critical organs around the tumor. However, the intensive use of ionizing radiation in clinical practice is also associated with the risk of radiological accidents, unjustified exposure, and undesirable side effects. In such situations, physical methods of dose estimation are not always possible or of low value. This is because the doses of radiation that cause side effects are different for individuals. In these cases, biological dosimetry is the best way to estimate the absorbed dose.

Cytogenetic analysis can be used to determine both the dose received and the individual radiosensitivity. Sensitivity to ionizing radiation can be an important indicator in providing protection against unjustified exposure (by individualised treatment) and in predicting side effects that occur after radiotherapy or a radiological accident. There is a proven link between increased levels of chromosomal damage and an increased risk of cancer. However, the Dicentric Chromosome Assay (DCA) is considered as the gold standard method for biological dosimetry and there is no consensus on whether the dose determined by this method depends on individual radiosensitivity.

This cytogenetic analysis for six prostate cancer patients was done to compare delivered and biologically evaluated doses by DCA, to see if the result of this assay will differ depending on estimated individual radiosensitivity by using G2-assay. This work is important for future research projects that may help to improve radiotherapy procedures by individualizing treatment plans or in the case of radiological incidents in clinical practice.

The study was conducted with the permission of the Lithuanian Bioethics Committee (bioethical permission to perform the biomedical research on chromosomal damage in lymphocytes (No. L-14-07/1)).

The aim – to investigate the impact of radiosensitivity on the patient’s estimated dose during radiotherapy treatment using cytogenetic analysis methods.

The tasks:

1. To evaluate the absorbed doses of patients' blood samples prior to radiotherapy treatment by using DCA and to compare with the delivered dose.
2. To determine the absorbed dose of patients after radiotherapy treatment by using DCA and to compare with total delivered dose during radiotherapy.
3. To assess individual radiosensitivity of patients prior and after radiotherapy treatment and to compare with results of DCA.

1. Literature Review

This section provides an analysis of the theory and research that is directly relevant to the topic.

1.1. Ionizing Radiation

Ionizing radiation is a stream of subatomic particles and photons having sufficient energy to cause ionization of atoms (to release electrons from atoms). This radiation can be:

- High energy electrical particles such as electrons and positrons (β radiation), He nuclei (α radiation), other nuclei.
- Neutral particles – photons (ultraviolet, X-ray and γ radiation) and neutrons.

Ionization of an atom is possible when the energy of the radiation particles or secondary particles is greater than the ionization energy of the atom, which is equal to the minimum binding energy of the electrons of the atom. This energy is usually in the order of 10 eV [1, 2].

The higher the energy of the ionizing particle, the greater the effect of ionizing radiation. Ionizing radiation's energy can be transfered to the substance and it is described by linear energy transfer (LET). LET is expressed in units of kiloelectronvolts per micrometre (keV/μm) or megaelectronvolts per centimetre (MeV/cm). Low LET – γ, X-rays and β radiation. High LET – He nuclei (α radiation), other nuclei, protons, neutrons.

1.2. Dosimetry

Ionizing radiation interacts with matter and transmits its energy to it. Basic dosimetric values [3]:

Absorbed dose is a physical value used to assess the effects of ionizing radiation. It is the amount of ionizing radiation energy absorbed by a material per unit mass:

$$D = \frac{dE}{dm} = \Psi \left(\frac{\mu_e}{\rho}\right)_E \quad (1.2.1)$$

where dE is the energy absorbed by the volume of the mass dm; Ψ- energy inflow; μ_e – linear energy absorption coefficient; ρ is the density of the material.

The unit of absorbed dose is gray (Gy). 1 Gy is equal to 1 J/kg. Non-systemic unit of absorbed dose is rad. 1 rad = 0.01 Gy.

The absorbed dose depends on the duration of irradiation. The absorbed dose per unit time is called the absorbed dose rate. The unit of measurement for this quantity is Gy/s or rad/s:

$$\dot{D} = \frac{dD}{dt} \quad (1.2.2)$$

where *dD* is the absorbed dose; *dt* – time.

Equivalent dose. The biological effects of ionizing radiation also depend on the type of radiation (α, β, γ, neutrons, nuclei, ions, etc.) and the energy of the particles. In other words, the ionization density is the number of electron and positive ion pairs that form in the path unit of the ionizing particle as it passes through the material. To determine the biological effect of radiation, the absorbed dose is

multiplied by a weighting factor k, which determines how many times the biological effect of a given type of radiation is greater than the biological effect of the 200 keV energy γ quanta. For example, the quality factor for γ radiation is 1 and for α radiation (<10 MeV) it is 10. The equivalent dose is calculated:

$$H = D \cdot k \tag{1.2.3}$$

where D is the absorbed dose; k is the quality factor.

The SI unit for an equivalent dose is the sievert (Sv). The non-systemic equivalent dose unit is rem (otherwise known as the biological X-ray equivalent). 1 rem = 0.01 Sv.

Effective dose is a measure of radiation exposure to a living organism when used in an uneven manner in the organs and tissues of the human body. This is the sum of the tissue equivalent doses multiplied by the tissue weighting factor wT:

$$H_e = \sum_T w_T \cdot H_T \tag{1.2.4}$$

where H_T is the mean equivalent dose in the T-organ or tissue; w_T is a weighting factor that indicates the effect of a particular tissue or organ on the onset of adverse effects in the body when the body is irradiated evenly. The highest weight ratio is in the gonads.

1.2.1. Dose Assessment

The three main dose assessment methods are shown in Figure 1.

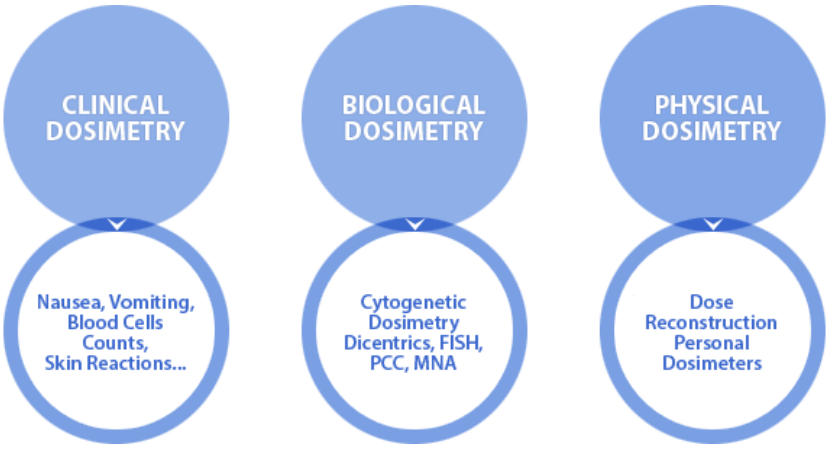

Fig. 1. Clinical, biological and physical dosimetry [4]

Physical devices for recording ionizing radiation are called **dosimeters**, which consist of a detector and measuring equipment. In radiation-sensitive volume of the detector, the ionizing radiation energy is converted into a signal which is convenient for recording. There are two kinds of dosimeters [5, 6, 7, 8]:

– **Passive Dosimeters** are integrating dosimeters that only provide an estimate of the total cumulative exposure. The examples of these dosimeters are:

- **Luminescent detectors.** Luminophores can store absorbed ionizing radiation energy. When illuminated by ultraviolet (photoluminescent dosimeters – FLD), visible light (optically stimulated luminescence dosimeters – OSL) or heating (thermoluminescent dosimeters – TLD), the absorbed energy is emitted in the form of a flash of light.
- **Radiographic detectors.** The photosensitive emulsion contains silver bromide AgBr or silver chloride AgCl. Gamma rays falling into the dosimeter generate secondary electrons that interact with AgBr and neutralize positive silver ions. Thus, on the surface of the grains appear centers of development – silver atoms.
- **Radiochromic dosimeters** are solid-state detectors that change color (due to polymerization) when exposed to ionizing radiation [9].

– **Active Dosimeters.** An active dosimeter gives a real-time measurement of the dose detected. The examples:

- **Gas detectors** are capacitors in which the space between the electrodes is filled with gas and in which an ionisation process takes place. The properties of these detectors are determined by the strength of the electric field and the distribution in space between the electrodes. If the generated field strength E is not sufficient for impact ionization, such detectors are called ionization chambers. Detectors that use shock ionization are called gas discharge meters or Geiger and Mueller meters.
- **Semiconductor detectors**. As in a gas ionization chamber, ionizing radiation creates pairs of positive and negative charge carriers that, when exposed to an external electric field, drift toward the respective electrodes and generate an electric current at the load resistance.
- **Scintillation detectors**. It is a nuclear particle counter consisting of a scintillator, a photomultiplier and an electronic system. The most commonly used are inorganic crystals (sodium iodide), organic liquids and plastics.

There are many studies that compare physical and biological dosimetry (see subsection 1.7.1.) methods. These evaluations of different dosimetry types are very important for establishing the radioprotective procedures and minimizing the risks to human health.

1.3. Radiotherapy

Radiotherapy is a one of the cancer treatment methods where ionizing radiation is used to kill cancer cells. There are two main types of radiotherapy: external (teletherapy) and internal (brachytherapy). The most commonly used device for external beam radiotherapy is a medical linear accelerator (LINAC). It uses high energy X-rays or electrons. Teletherapy machines with Co-60 source, which emits gamma rays, are also used in many countries. Heavy ions, protons, neutrons and etc., that are generated in specific accelerators like cyclotrons, are also used in radiotherapy in some countries [10, 11].

Clinical X-ray beams have an energy range of 10 kVp to 50 MV and are generated by decelerating electrons with kinetic energies of 10 keV to 50 MeV in special targets. Clinical X-ray equipment operates in the range of:

– Superficial (10 kVp–150 kVp)
– Orthovoltage (150 kVp–400 kVp)

– Megavoltage electron accelerators (for X-ray and electron therapy)

From Figure 2 it is clear that in the case of X-ray beams the relative deposited energy has a maximum value at a shallow tissue depth [12, 13]. The difference between superficial and megavoltage X-rays is also seen. And, for example, positive charged particles like protons and heavy ions "…have more favourable intrinsic physical properties displaying a finite adjustable range ("zero" exit doses) and an inverse depth dose profile (Bragg peak), which reduces entrance dose to about 50% of the dose delivered in a clinically relevant target." [11]. Moreover, when compared to low LET radiation, charged particle radiation has been proven to be more effective in inducing chromosomal abnormalities [13, 14].

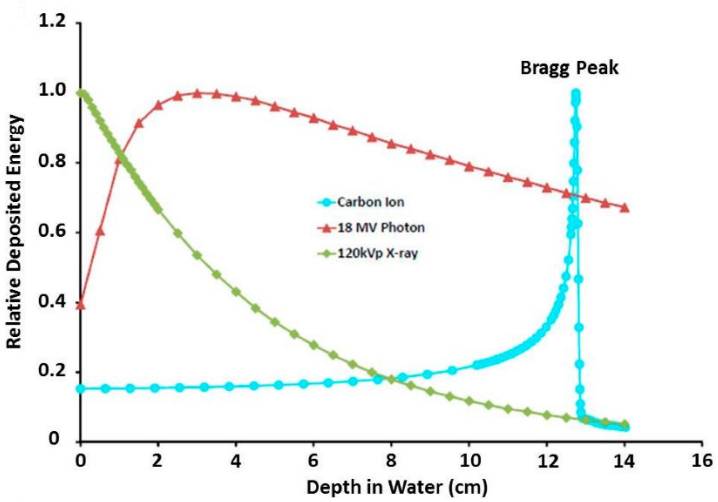

Fig. 2. The relative deposited energy as a function of depth in water for particle (Carbon ion) and photon beams [13]

Medical linacs are accelerators that use microwave RF fields to accelerate electrons in accelerating waveguides, following straight trajectories. So, electrons travel in a straight line via the same, low potential difference multiple times. Photon energies of 6 and 18 MV and many electron energies are provided by a typical modern high energy linac [10].

With the evolution of delivery systems, the opportunity to adjust dose to unique shaped targets has risen significantly, from 2D-RT to 3D-RT to IMRT, VMAT, and stereotactic RT. Due to enhanced precision in patient placement and improved techniques to deal with organ motion (image guided RT (IGRT)), the margins between planned target volumes (PTV) and clinical target volume (CTV) have been reduced [11].

Intensity modulated radiation therapy (IMRT) is a type of 3D treatment. The intensity of the beams may be modified to reduce the dose reaching surrounding normal tissues, in addition to shaping and targeting them towards the tumor from various angles. This method is most commonly employed when tumors are located near important structures.

Volumetric modulated arc treatment or RapidArc technique (VMAT) is a form of IMRT. It uses a machine that rapidly spreads radiation over the body while rotating. (Fig. 3) [15, 16]. "Compared with conventional radiation therapy and IMRT, VMAT gives more accuracy and less damage to the surrounding tissue with better advantage." [17].

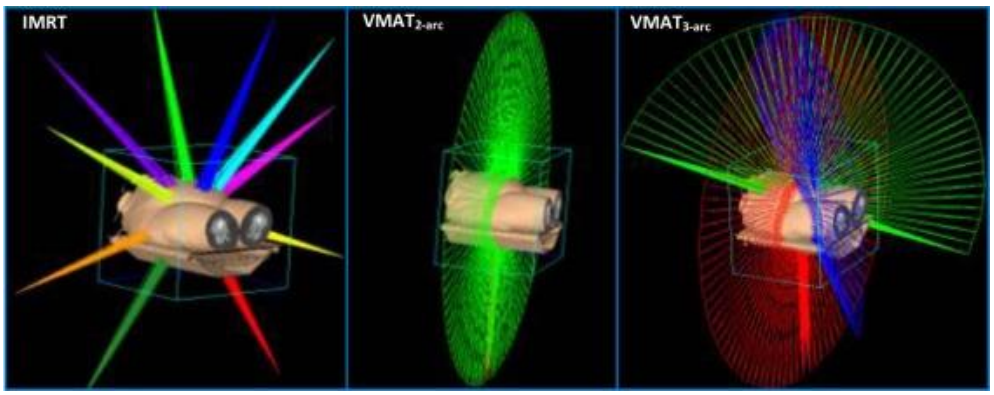

Fig. 3. IMRT vs VMAT [16]

1.3.1. Treatment Planning Systems

Treatment planning systems (TPS) are the fundamental part of radiotherapy. After loading the image datasets and identifying the tumors, the systems develop a sophisticated plan for how the therapy system will radiate the tumor. The software calculates the predicted dose distribution in a patient's tissues, including variables such as tissue energy level penetration. These systems also help orient the beam in the arrangement, avoiding critical structures. It can include automated, sophisticated multi-leaf collimator (MLC) leaf sequence programming to form a beam around critical structures during dose administration [18].

The most important software component in a computerized TPS are the dose calculation algorithms. These modules are responsible for accurate representation of the dosage in the patient. By tracking the paths of a huge number of particles as they travel from the source of radiation and undergo numerous scattering interactions both within and outside the patient, Monte Carlo or random sampling techniques are used to derive dose distributions [10].

According to ICRU Report No. 50, target dosage uniformity should be within +7% and –5%. ICRU Reports No. 50 also describes target and critical structure volumes for the treatment planning (Fig. 4) [10, 19]. For example:

- "The Gross Tumour Volume (GTV) is the gross palpable or visible/ demonstrable extent and location of malignant growth" [19]. The GTV is generally determined using imaging modalities, such as CT, MRI, ultrasound, etc.
- "The clinical target volume (CTV) is the tissue volume that contains a demonstrable GTV and/or sub-clinical microscopic malignant disease, which has to be eliminated. This volume thus has to be treated adequately in order to achieve the aim of therapy, cure or palliation" [19].
- "The planning target volume (PTV) is a geometrical concept, and it is defined to select appropriate beam arrangements, taking into consideration the net effect of all possible geometrical variations, in order to ensure that the prescribed dose is actually absorbed in the CTV" [19].

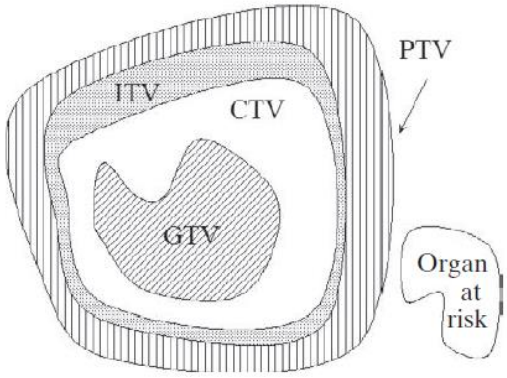

Fig. 4. Volumes of interest in radiotherapy [10]

1.4. Prostate Cancer

When the cells in the prostate gland change and begin to divide uncontrollably and concentrate in a tumor, prostate cancer occurs. (Fig. 5). Some prostate tumors grow very slowly, so a person does not feel any symptoms for a long time. Large number of prostate cancer cells begin to produce too much of a prostate-specific antigen (PSA). This type of cancer differs from other types of cancer since it is concentrated (almost without any spread from the prostate). If the cancer is distributed in a form of metastasis to other organs, the disease can't be controlled, and causes pain and other symptoms [20].

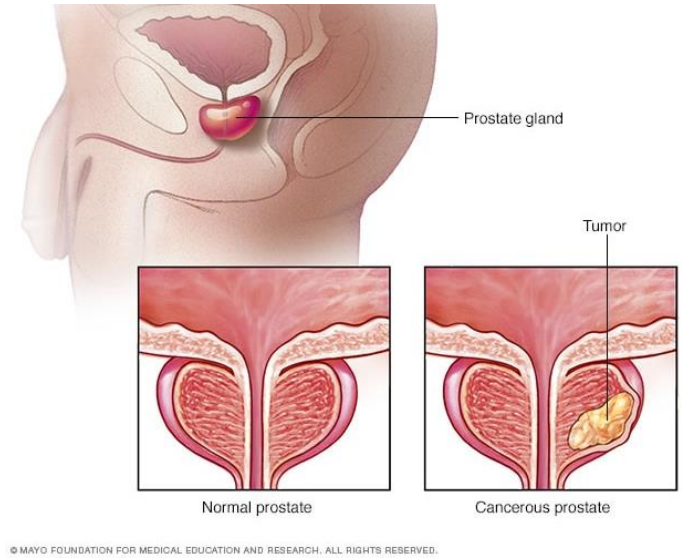

Fig. 5. Cancerous prostate [21]

The test to identify prostate cancer involves taking blood from a vein and determining the level of prostate-specific antigen in the blood. If the PSA level exceeds 3ng/ml, prostate cancer is suspected. High levels of PSA may be a sign of prostate cancer, but this protein may also increase due to other prostate diseases, such as infection, benign prostatic hyperplasia, and other prostate irritations [22].

Predicting the best treatment for prostate cancer for a particular patient is not always straightforward, as the impact of many factors needs to be assessed. The types of prostate cancer treatment are different. For example, external beam therapy, brachytherapy, surgery. If prostate cancer has spread to other organs, hormone therapy is used. Hormone treatment does not kill the cancer, but the body lowers testosterone, and the disease is controlled for a long time. Another way to reduce testosterone levels is to remove the testicles (surgical castration or orchidectomy). Testosterone is mainly

produced by the testicles. Removal of the testicles rapidly lowers testosterone levels and successfully controls the disease [20].

Numbers of new cancer cases in 2020 in Lithuania are presented in Figure 6.

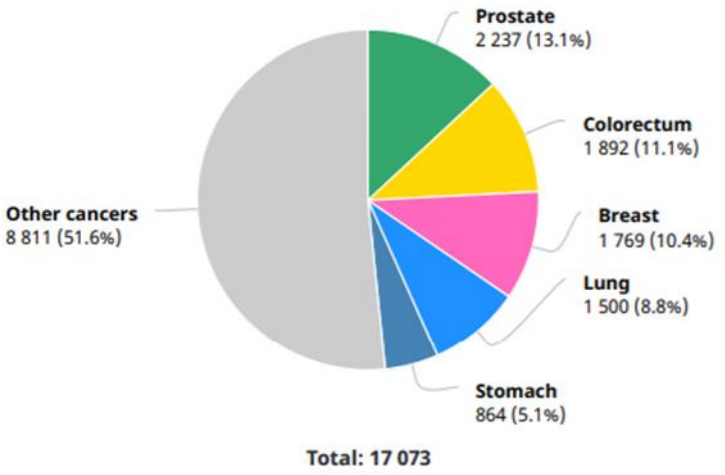

Fig. 6. Numbers of new cancer cases in 2020, both sexes, all ages in Lithuania [23]

1.4.1. External Beam Radiotherapy for the Prostate Cancer Patients

Radiotherapy is used to treat the whole tissue. Its goal is to eliminate all cancer cells, including those that have spread to the prostate. Radiation therapy can be given to a larger area, including neighboring lymph nodes, if there is a possibility that the cancer has spread there. Lymph nodes are present all over the body and are part of the immune system. Prostate cancer frequently spreads to the lymph nodes in the pelvic area. Side effects are more likely to occur when radiation is applied to a larger area [24].

In the early stages of prostate cancer, a radiation dose of 70.2 Gy or a higher dose of 79.2 Gy can be employed. After surgery or at a later stage of cancer, a booster dose can be given. Rectal bleeding, diarrhea, hematochezia, radiation cystitis, radiation proctitis, etc. are possible side effects [17].

1.5. Radiobiology

“Radiobiology, a branch of science concerned with the action of ionizing radiation on biological tissues and living organisms, is a combination of two disciplines: radiation physics and biology.” [10]

Radiation-induced cell death is primarily caused by deoxyribonucleic acid (DNA) damage. The actions can be of two types: **direct (20–30%)** and **indirect (70–80%)** (Fig. 7). The effects (physical and chemical) of ionizing radiation described below are **indirect**.

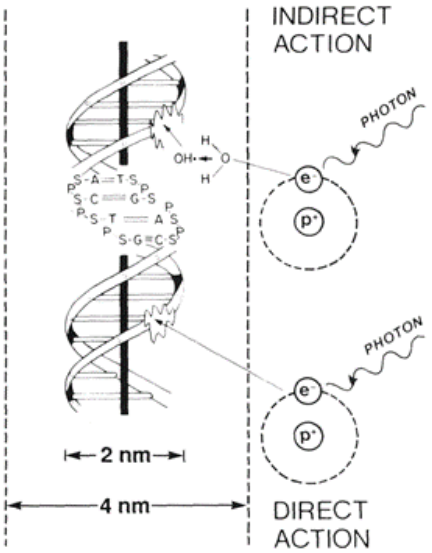

Fig. 7. Indirect and direct actions of ionizing radiation [25]

"Irradiation of biological systems generates a succession of processes that differ in time-scale. These processes are divided into three phases" [26] (Fig. 8).

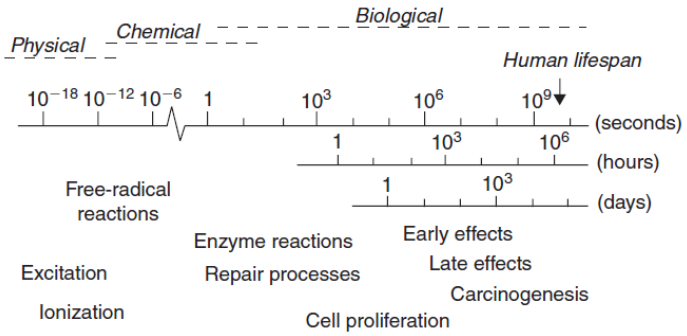

Fig. 8. Time-scale of the physical, chemical, biological effects caused by ionizing radiation exposure on biological systems [26]

In the first process (physical), the tissue molecules are ionized and excited. In the second stage (chemical), chemically active products are formed: ions and free radicals.

75% of the human body weight is water. When water is irradiated, electrons escape from the water molecules and positive, negative molecular ions and interacting radicals are formed. The main cause of radiation exposure is the radicals H^+, OH^- and especially hydroperoxide HO_2. These compounds interact with the molecules of organic matter, oxidizing and decomposing them.

All later processes are included in the third stage, the biological phase. The majority of lesions in DNA (Fig. 9) are repaired effectively. Some lesions can't be healed , and these are the ones that lead to cell death. Cells can take a long time to die. Even receiving a small dose of radiation, they may

go through several mitotic divisions before dying.

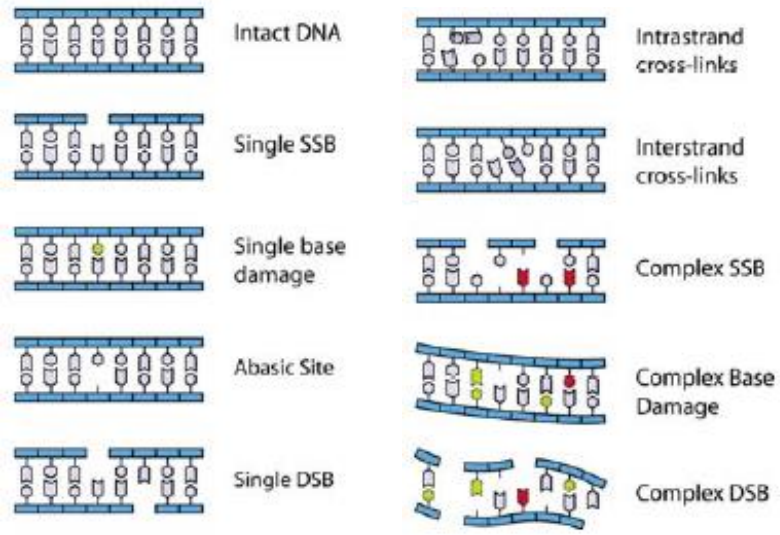

Fig. 9. Radiation induced DNA lesions (SSB – single strand break, DSB – double strand break) [27]

Direct action is when an ionizing particle interacts with macromolecules in a cell (DNA, RNA, protein, etc.) and these macromolecules develop aberrant structures that lead to biological changes [25].

DNA repair systems ensure that most of the damages will be repaired. However, incorrect DNA repair can lead to an increase **in mutations, chromosomal aberrations, genetic instability, cell death, and cancer**. The basic principles on which the genetic risk assessment of ionizing radiation is based are the following: Mutations in germ cells caused by ionizing radiation lead to the same genetic diseases as spontaneous mutations. Ionizing radiation usually does not induce specific mutations unique to ionizing radiation but increases the frequency of spontaneous mutations. "When estimating the genetic radiation risk, a doubling dose of 1 Gy is assumed in the case of chronic exposure. This means that a dose of 1 Gy doubles the spontaneous frequency of all clinically dominant mutations which is about 2% per generation. In the case of acute radiation exposure the doubling dose is 0.3 Gy." [28].

The early indications of tissue damage during the first weeks or months following ionizing radiation exposure are caused by the destruction of stem cells. Cell proliferation, which occurs in both normal tissues and tumors, is a secondary effect of cell death. **Late reactions** appear at later times after the irradiation of normal tissues. Skin fibrosis and telangiectasia, spinal cord injury, and blood vessel damage are all examples. The emergence of second tumors (i.e. radiation carcinogenesis) is an even later symptom of radiation damage. As a result, the detectable effects of ionizing radiation might last for several years after exposure.

In other words, unwanted or harmful effects of ionizing radiation may be stochastic or deterministic. A stochastic effect is one in which there is no threshold dose for side effects (but probability of these harmful effects to occur increases with increasing dose). A deterministic effect increases in intensity with increasing dose.

To conclude, irradiation of a cell will result in such outcomes [10]:

- There is no effect.
- The cell's division has been delayed.
- Apoptosis: The cell dies before it can divide.
- Reproductive failure: When a cell attempts its first or subsequent mitosis, it dies.
- Genomic instability: Induced genomic instability causes a delayed kind of reproductive failure.
- Mutation: Although the cell survives, it has a mutation.
- Transformation: The cell survives, but the mutation results in a transformed phenotype and the possibility of cancer.
- Bystander effects: Irradiated cells can send signals to unirradiated cells nearby, causing genetic harm.
- Adaptive responses: Irradiated cells are stimulated to become more resistant to irradiation.

1.5.1. Radiobiology Impact in Radiotherapy

Ionizing radiation causes side effects in patients undergoing medical imaging and radiotherapy procedures. However, the diagnostic / treatment value of the procedure can be higher than the risk of radiation injury.

There are five biological factors called the five Rs of radiotherapy:

1. **Radiosensitivity.** The radiosensitivity of mammalian cells is known to be unequal. The law of J. Bergonie and L. Tribondeau states that the radiosensitivity increases with increasing rate of cell division and decreases with increasing degree of differentiation, i.e., the more specialized the cells are in certain functions, the less radiosensitive they are [29]. Bone marrow, genital and gastrointestinal mucosal cells are highly radiosensitive, and nerve, muscle and bone tissue and liver cells are less radiosensitive. In other words, there is a significant difference in radiation response between early responding tissues, for example skin, and late responding tissues, for example spinal cord. (Fig. 10). Late responding tissues' cell survival curves are more curved than those of early responding tissues. The α/β ratio is high for early effects, and α/β is low for late effects. For early and late effects α/β = 10 Gy and α/β = 3 Gy, respectively. Both **tumor cells** and early responding tissues‘ cells exhibit similar values (α/β = 10 Gy) [10].

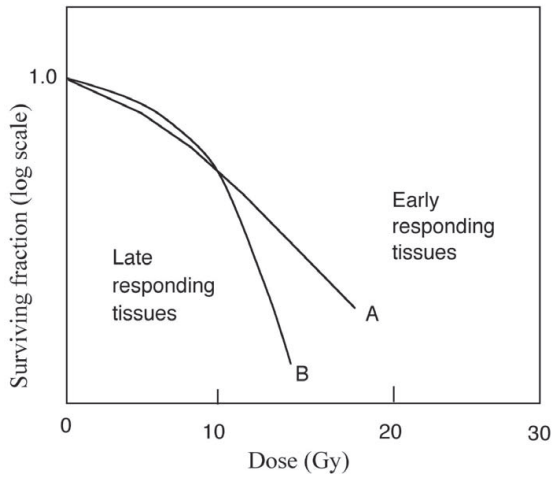

Fig. 10. Hypothetical target cell survival curves for early responding tissues (curve A) and late responding tissues (curve B) [10]

2. **Repair.** Because sublethal damage repair occurs throughout the extended exposure, radiation supplied at a lower dose rate may result in less cell death than radiation delivered at a higher dose rate for the same radiation dosage. The typical dose rate used in standard radiotherapy is 1 Gy/min [10].
3. **Repopulation.** Cells can repopulate while receiving fractionated doses. A greater therapeutic ratio is achieved by fractionating radiation treatment such that it is delivered across several weeks rather than in a single session. However, the total dose in a fractionated therapy must be substantially higher than the dose in a single treatment to achieve the necessary degree of biological damage [10].
4. **Redistribution.** After fractional treatment, redistribution in proliferating cell populations at all stages of the cell cycle enhances cell death relative to a single treatment session. The cell proliferation cycle is divided into two parts: mitosis (M), which is when the cell divides, and DNA synthesis (S). The S and M phases are separated by G_1 and G_2 gaps. The S phase of mammalian cells grown in culture is usually in the range G_2 lasts 2–4 hours, G_1 lasts 1–2 hours, and M lasts less than an hour. The whole cell cycle is on the order of 10–20 hours (another set of time values are presented in Fig. 11). The cell cycle of stem cells in certain tissues, on the other hand, can last up to ten days. The M and G_2 phases of the cell cycle are the most radiosensitive, while the late S phase is the most resistant. Malignant cells have a shorter cell cycle than some normal tissue cells, while normal cells can proliferate quicker during regeneration following injury.

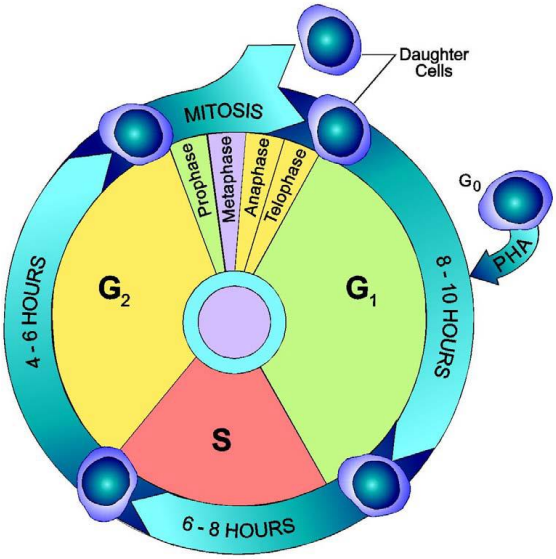

Fig. 11. The cell cycle [27]

5. **Reoxygenation.** During a fractionated course of treatment, hypoxic cells are reoxygenated, and become more radiosensitive. The biological effect of ionizing radiation is influenced by the presence or lack of molecular oxygen within a cell. This is because oxygen is actively involved in the formation of hydroperoxides and peroxides.

The purpose of radiotherapy is to deliver enough radiation to the tumor to kill it while avoiding irradiating healthy tissues to a level that may cause major complications (morbidity). The theory is commonly demonstrated by drawing two sigmoidal curves, one for tumor control probability (TCP) (curve A) and the other for complication of normal tissues probability (NTCP) (curve B), as shown

in Figure 12. In the treatment of a particular tumor, the best radiation dose delivery approach is one that optimizes TCP while simultaneously minimizing NTCP.

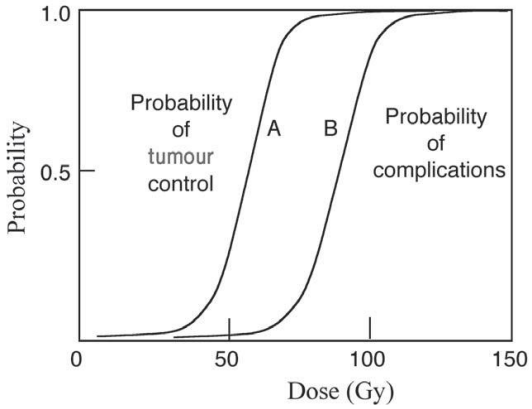

Fig. 12. Curve A represents the probability of tumour control and curve B the probability of complications. [10]

Various chemical agents can affect a cell's reaction to ionizing radiation, either decreasing or increasing it. Radioprotectors are chemical agents that inhibit the cell's sensitivity to radiation. By scavenging the creation of free radicals, they generally influence the indirect effects of radiation. Radiosensitizers are chemical compounds that improve cell sensitivity to radiation and generally stimulate effects of radiation. [10].

1.6. Radiation Induced Chromosome Damage and Biological Dosimetry

The nucleus of the cell contains chromosomes that consist of DNA and proteins forming a thread-like structure (Fig. 13).

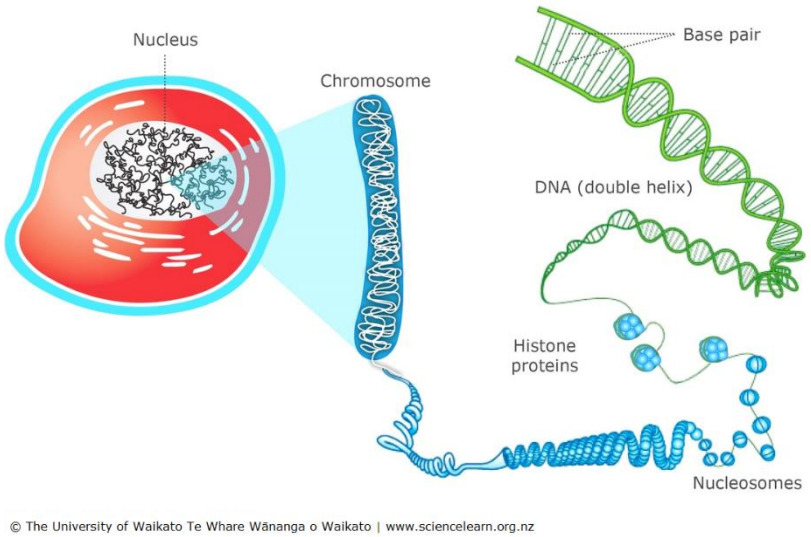

Fig. 13. Cell, chromosome and DNA [30]

The human karyotype (Fig. 14) is the characteristic chromosome complement for humans that consists of 23 pairs of chromosomes of various sizes, totaling 46 chromosomes in each cell [27].

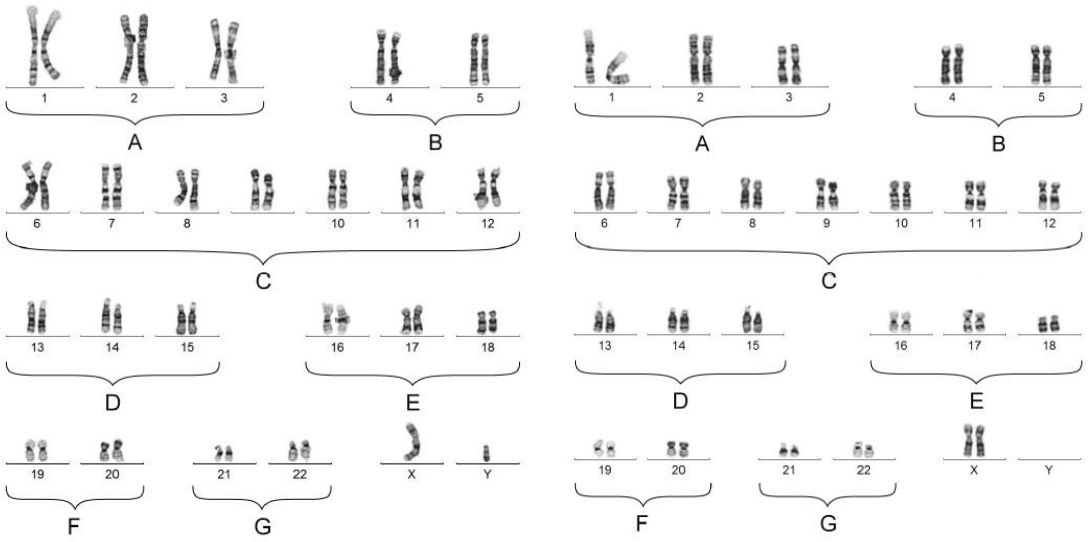

Fig. 14. A banded chromosome/karyotype preparation from a normal male XY (left) and a normal female, XX (right) [27]

It is clear that the effects of ionizing radiation to humans and living organisms depend on the amount of energy absorbed, e.g., an annual absorbed dose of 1 mGy causes about 1016 ionizations, i.e., 100 ionizations per cell and an average of one ionization per DNA molecule. A dose of 1000 mGy of gamma radiation causes about 1000 single-stranded DNA breaks, 40 double-stranded DNA breaks, 150 DNA-protein cross links, and thousands of other lesions [31]. Chromosome aberrations occur when double-stranded DNA breaks occur.

When DNA repair is incomplete, chromosomal damage might occur. Rings, dicentrics, translocations, and other chromosomal abnormalities occur when broken ends reconnect with other broken ends (Fig. 15).

Dicentrics and rings are unstable aberrations that destroy the cell and, as a result, are not passed down to the next generation. Because cells which were exposed have a finite lifetime and are eliminated, the incidence of dicentrics and rings decreases over time.

Translocations are stable aberrations that can last for years since they are not lethal to the cell and are passed down through the generations. However, when translocations have taken place in germ cells, the child may experience an increase in genetic consequences.

Radiation exposure can be detected by structural chromosomal abnormalities. Biodosimetry involves assays to determine the radiation dosage based on the type or frequency of chromosomal abnormalities in the cells which were exposed. Biodosimetry has shown to be a valuable method for determining doses in circumstances of known or suspected acute (unwanted) radiation exposure.

Numerous human and animal studies have shown that exposure to blood at the same dose both in vivo and in vitro induces similar levels of chromosomal damage. Therefore, the resulting exposure dose can be determined by comparing the amount of chromosomal damage in the blood of irradiated humans with an in vitro calibration dose-response curve [27, 32].

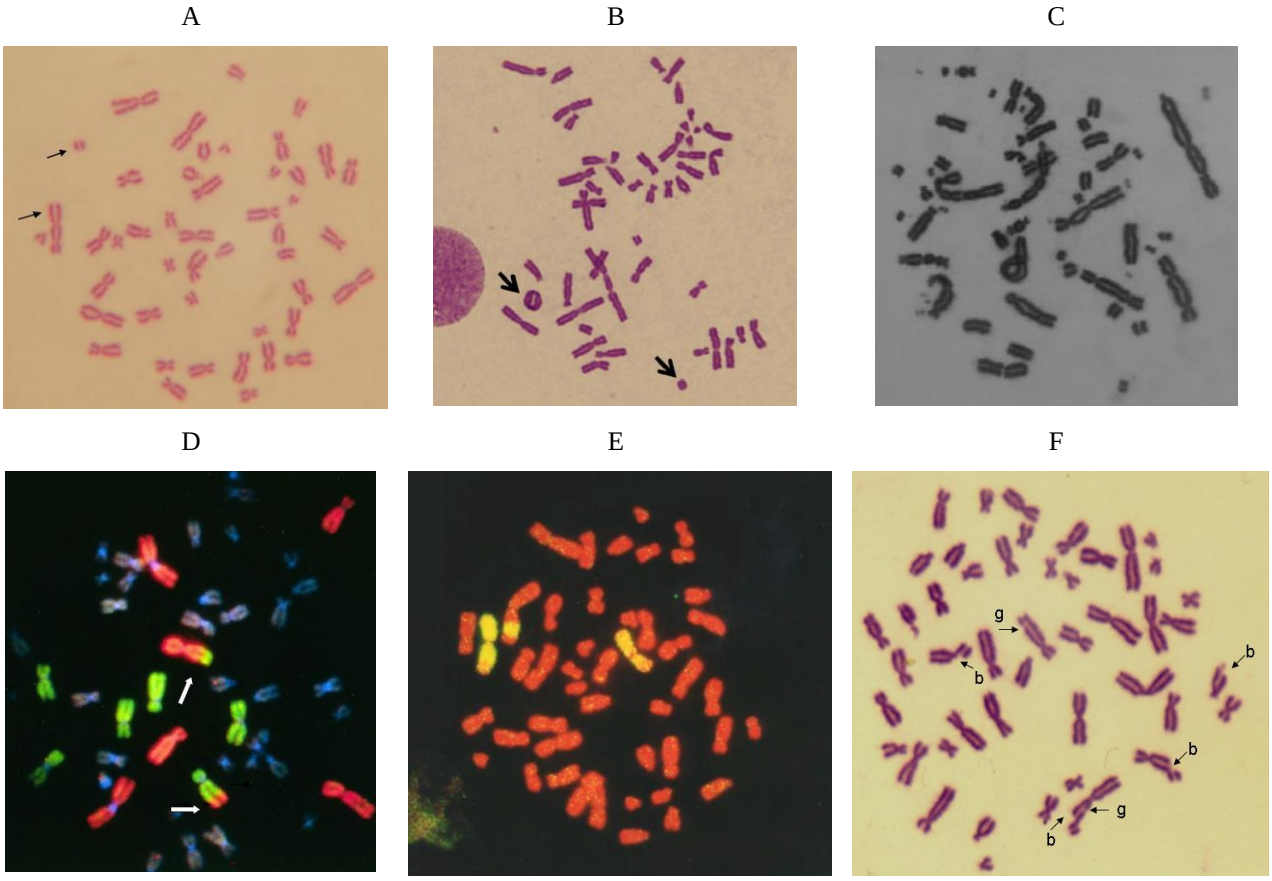

Fig. 15. Chromosome-type aberrations (unstable): A – dicentric chromosome with its accompanying acentric fragment, B – a metaphase spread with two rings, C – a rogue cell. Chromosome-type aberrations (stable): D – reciprocal translocations, E – interstitial translocations (insertions). Chromatid-type aberrations: F – a metaphase spread with chromatid breaks (b) and gaps (g) [27]

Type of cytogenetic damage depends on which phase of cell cycle irradiation occurs:

- Chromosome aberrations:
  - G_1 or G_0 irradiation.
  - Both chromatids are involved.
  - Dicentrics, centric rings, rogue cells, translocations.
- Chromatid Aberrations:
  - S or G_2 irradiation.
  - Usually, one chromatid is involved.
  - Terminal and interstitial deletions, achromatic lesions, isochromatid deletions, asymmetrical and symmetrical interchanges.

UV and chemicals induce usually induce chromatid aberrations.

Comparison of cytogenetic aberration assays used for biodosimetry is presented in Table 1.

Table 1. Comparison of cytogenetic aberration assays [27, 33]

	Premature chromosome condensation (PCC)	**Dicentric (and ring) (DCA)**	**Fluorescent in situ hybridization (FISH)**	**Cytokinesis-block micronucleus (CBMN)**
Typical aberrations	excess chromosome fragments; dicentrics and rings translocations	dicentrics (and rings)	dicentrics (and rings) translocations	micronuclei nucleoplasmic bridges
Typical radiation scenario applications	acute recent exposure	acute protracted recent exposure	acute protracted old exposure	acute protracted recent exposure
Photon equivalent, acute dose range (Gy) for whole-body dose assessment	0.2 to 20	0.1 to 5	0.25 to 4	0.3 to 4
Useful for partial body exposure applications	Yes	Yes	Not available	Not available
Useful for triage dose assessment	Yes	Yes	Not available	Yes
Time since exposure	days	days; months	days; months; years	days; months
Time (h) from sample receipt to dose estimate	2	52–55	120	75

The dicentric assay was the only method of biological dosimetry for many years, and it is still the most widely used technique today [34, 35]. There are now a variety of different biological endpoints that can be measured in lymphocytes [27].

There are several reasons why peripheral lymphocytes are used for biological dosimetry. The fact that the majority of peripheral lymphocytes are part of the 'redistributional pool' is critical for interpreting irradiation induced chromosomal abnormalities in humans. The average period a redistributional pool lymphocyte is present in the peripheral circulation is around 30 minutes. This indicates that lymphocytes with chromosomal abnormalities created everywhere in the body will eventually reach the peripheral blood [27, 36].

The sensitivity of different phases of the cell cycle to chemicals or radiation varies, and the forms of chromosomal aberration caused differ based on the cell stage that was treated. As a result, working with a synchronized population is important in such investigations. The majority of mitogenically activated peripheral lymphocytes do not cycle and are at the G_0 stage of the cell cycle. The initial cell cycle after stimulation in lymphocytes is nearly synchronized, making these cells ideal for radiobiological research [27].

In summary, there is no single universal biological dosimetry method suitable for all cases of radiation exposure. Some methods, such as unstable chromosome aberration assay in peripheral blood

lymphocytes, suitable for acute or for relatively recent exposures, others, such as the FISH method, are suitable to investigate past exposure.

It is important to note that changes in chromosomal structure have been demonstrated to have a significant effect in carcinogenesis. Protooncogenes can be activated or genes that suppress tumor development can be inactivated in the presence of chromosomal abnormalities [37]. In epidemiological studies, cytogenetic biomarkers are employed to evaluate cancer risk. The majority of such studies show a clear relationship between increased chromosomal abnormalities and the risk of cancer [38, 39].

1.7. Dicentric Chromosomes

Ionizing radiation produced by dicentric chromosome formation due to mis-rejoining of DNA double strand breaks formed on two chromosomes is shown in Figure 16. Acentric pieces generally follow dicentric chromosomes.

DCA starts from obtaining peripheral blood from individuals that are exposed to radiation. Then lymphocytes are stimulated to grow and cells in first division metaphase spreads are collected. Finally, cells in this stage are analyzed for chromosome aberrations. By counting the frequency of dicentric chromosomes and comparing with calibration curves reflecting radiation quality, the dose is estimated [40]. This method allows the evaluation of the absorbed dose from 0.1 Gy to 5 Gy.

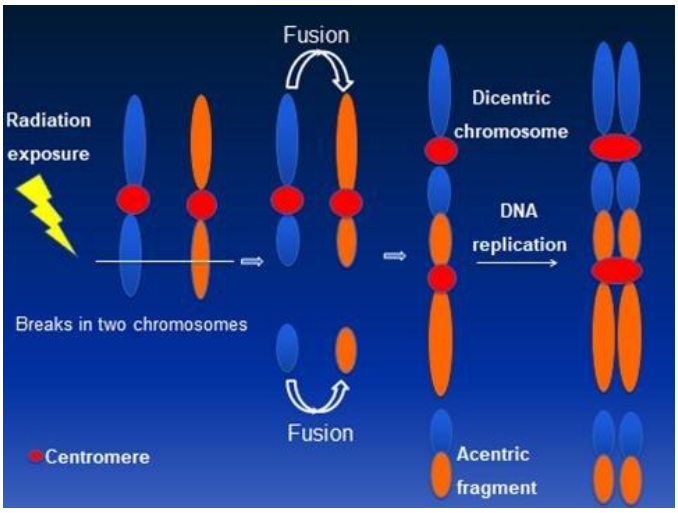

Fig. 16. Formation of dicentrics [41]

DCA is technique dependent and time consuming. However, background level for dicentrics is low in the sample, so it is specific for radiation. There are some factors that effect the results of DCA [40]:

- Total absorbed dose.
- Dose rate.
- Percent body irradiated.
- Radiation quality.
- Sampling time after exposure.

Optimal time for the blood sample collection is between 24 hours and 4–6 weeks after ionizing radiation exposure.

Radiation quality is important for dose assessment. The acts of ionization of low LET particles are randomly distributed among cells. Thus, the damage caused to the DNA molecules will be distributed in the cells randomly. Exposure to X-rays and γ-rays has been shown to cause an increase in chromosomal damage consistent with the Poisson distribution [27]. The acts of ionization of high LET are not randomly distributed among cells, the resulting energy is stored in discrete packets, and DNA and chromosome damage is unevenly distributed among cells. In this case, there will be more cells with multiple lesions and more cells without lesions than expected by the Poisson distribution. High LET electrical particles almost always interact several times with the same DNA molecule, causing formation of damage clusters that are resistant against reparation [27]. Dose dependence on the frequency of dicentric chromosome formation for high and low LET particles is shown in Figure 17.

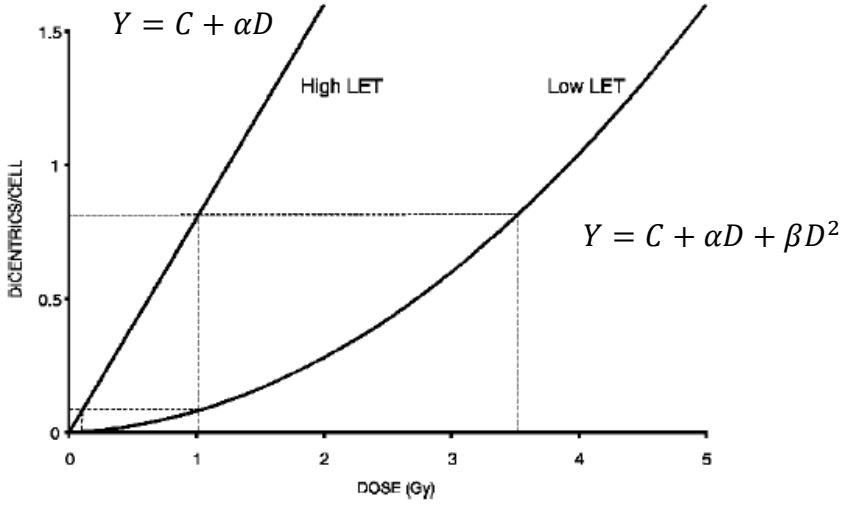

Fig. 17. Linear and linear quadratic dose response curves for high LET and low LET [27]

Another important measure is Relative Biological Effectiveness (RBE) which depends on the LET. "The relative biological effectiveness (RBE) compares the dose of test radiation to the dose of standard radiation to produce the same biological effect. The standard radiation has been taken as 250 kVp X-rays for historical reasons but is now recommended to be Co-60 γ-rays." [10]. As the LET increases, the RBE increases and reaches its maximum value at a LET of 100 keV/μm, after which the RBE starts to decrease (Fig. 18). At this ionization density, the average distance between the two ionization acts is 2 nm (the same as the DNA strand diameter), therefore there is a high probability that an electrical particle passing through DNA will cause a double break. Radiation that even more often ionizes the substance (when LET = 200 keV/μm) easily causes double-strand breaks, however, energy is "wasted" because the ionization acts are too close to each other.

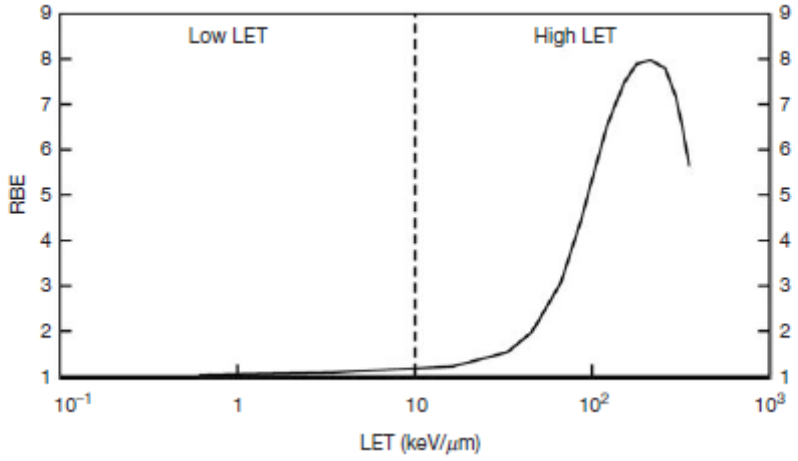

Fig. 18. RBE against LET [10]

Example data used to construct dose response curves for low and high LET radiations are presented in Table 2. There N – total number of cells scored; X – total number of dicentrics observed; σ^2/y – cell distribution of dicentrics and dispersion index; u – u-test. u values greater than 1.96 indicate overdispersion [27].

Table 2. Cytogenetic results obtained from blood samples irradiated with γ-rays and ^{4}He particles (α particles) [27]

γ-rays (Cobalt-60)

dose (Gy)	N	X	cell distribution of dicentrics							σ^2/y	u
			0	1	2	3	4	5	6		
0.000	5000	8	4992	8						1.00	-0.07
0.100	5002	14	4988	14						1.00	-0.13
0.250	2008	22	1987	20	1					1.08	2.61
0.500	2002	55	1947	55						0.97	-0.86
0.750	1832	100	1736	92	4					1.03	0.79
1.000	1168	109	1064	99	5					1.00	-0.02
1.500	562	100	474	76	12					1.06	1.08
2.000	332	103	251	63	17	2				1.14	1.82
3.000	193	108	104	72	15	2				0.83	-1.64
4.000	103	103	35	41	21	4	2			0.88	-0.84
5.000	59	107	11	19	11	9	6	3		1.15	0.81
Average										1.0	

20 MeV ^{4}He particles

dose (Gy)	N	X	cell distribution of dicentrics								σ^2/y	u
			0	1	2	3	4	5	6	7		
0.000	2000	3	1997	3							1.00	-0.04
0.051	900	19	881	19							0.98	-0.44
0.104	1029	27	1004	23	2						1.12	2.84
0.511	1136	199	960	154	21	1					1.07	1.60
1.010	304	108	217	69	15	3					1.09	1.15
1.536	142	96	75	40	25	2					0.98	-0.20
2.050	137	120	63	44	16	12	2				1.20	1.65
2.526	144	148	66	34	25	14	3	2			1.40	3.40
3.029	98	108	47	16	17	17	0			1	1.56	3.93
Average											1.19	

1.7.1. Applications of Biological Dosimetry

Biological dosimetry helps to evaluate the absorbed dose of ionizing radiation to humans, to distinguish between exposure to natural and artificial radiation, assess the risk of exposure, etc. But the most important application of biological dosimetry is the estimation of the magnitude of emergency exposure, providing medical personnel information about the exposure size received by

the human. This information helps to make decisions about treatment strategies, such as bone marrow or stem cell transplants. One of the most widely used methods for the determination of emergency exposure doses is the analysis of dicentric chromosomes which has been used in several radiation accidents, e.g., Chernobyl, Tokaimura, Fukushima [42–45].

In order to standardize the performance of cytogenetic studies, International Atomic Energy Agency (IAEA) recommendations were published [27]. International Organization for Standardization (ISO) has also approved a standard for laboratories performing biological dosimetry using cytogenetic assays (ISO 19238:2014) [46]. A separate standard validates the assessment of biological doses based on dicentric chromosome assays in the event of radiological and nuclear accidents (ISO 21243: 2008) [47].

On a European and worldwide level, many networks based on biological dosimetry have been formed. European Network of Biodosimetry "(RENEB) is a network founded within the 7th EU framework EURATOM Fission Programme. Beginning with 2016 a total of 26 organizations from 16 European countries have signed a Memorandum of Understanding (MoU) for mutual assistance in individual dose estimation in large scale radiological and nuclear emergencies" [48]. This network includes:

- Dicentric Chromosome Assay (DCA);
- FISH assay (FISH);
- micronucleus assay (MN);
- premature condensed chromosome assay (PCC);
- gamma-H2AX assay;
- gene expression assay;
- electron paramagnetic resonance (EPR);
- optically stimulated luminescence (OSL).

For example, in 2019, RENEB conducted a field exercise in Lund, Sweden, to replicate several real-world exposure scenarios. The DCA results were remarkably consistent across participants (Lithuania is included) and closely matched the reference dosage (95% of estimations were within ±0.5 Gy of the reference) (Fig. 19) [49].

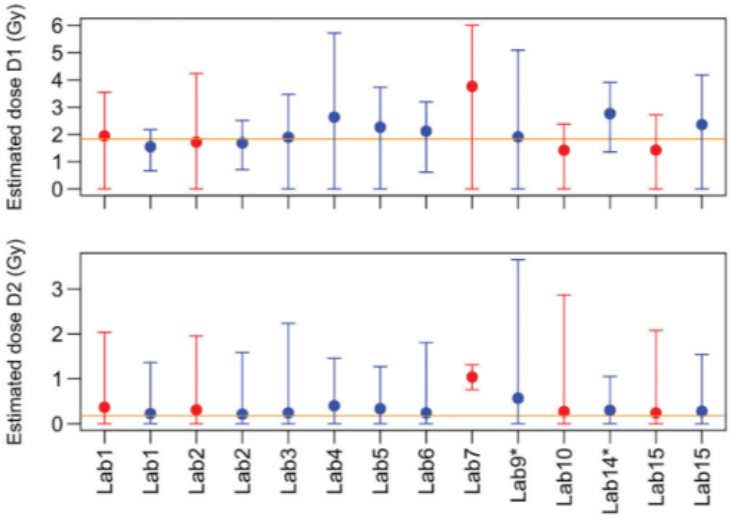

Fig. 19. Dose estimates for exposures with 95% confidence intervals. Red color – semi-automatically; blue color – manually scored results [49]

Another example is a previous study in which two intercomparisons were done among the participating laboratories. Between intercomparisons 1 and 2, the precision of dosage estimates improved, demonstrating the need to repeat such tests [50].

An international laboratory inter-comparison of eight biological dosimetry assays was organized in 2021. Variance in reported dose estimates varied between teams [51]

On the worldwide level – IAEA initiated a Response Assistance Network (RANET) in 2006 [52] and in 2007, the World Health Organization (WHO) created BioDoseNet, a global network of biodosimetry laboratories [53].

Since 2015 Lithuania is a member of the RENEB for preparedness and response to large-scale emergencies and participates in the network's comparative studies and preparedness testing exercises at various levels. Lithuania's RPC was involved in dose estimation of four different irradiated blood samples during an inter-laboratory comparison on DCA within the RENEB. The actual doses administered to the test samples were 0 Gy, 0.44 Gy, 1.08 Gy, and 1.89 Gy, while RPC dose estimates of 0.031 Gy, 0.505 Gy, 1.438 Gy, and 2.038 Gy respectively, showed tolerable accuracy [54].

DCA has certain shortcomings. The main problem of this assay is that that the frequency of dicentric chromosomes decreases over time because these aberrations are unstable and are eliminated by cell division. Using this method and knowing the decrease in dicentric chromosomes over time, an accurate assessment of the dose received can be performed within the first three years after exposure. However, after receiving a high (above 1 Gy) dose, reliable dose estimation time is less than one year [55].

Another problem – manually DCA is time consuming. The machine learning method can be used to identify dicentric chromosomes, with a true positive rate (TPR) of 50–65%. It is required to design a mechanism for increasing the rate and accuracy of identification [56]. A combined processing technique involving clustering and watershed was presented in one of the studies. The TPR of

dicentric chromosome identification was 76.6%, which was greater than the true positive rate of the threshold algorithm – 63.9% [57].

The frequency of dicentric chromosome formation in the sample depends on the scorer's experience. Figure 20 shows the data in chronological order and for each scorer. 6 Gy X-ray dose was given to each sample [58].

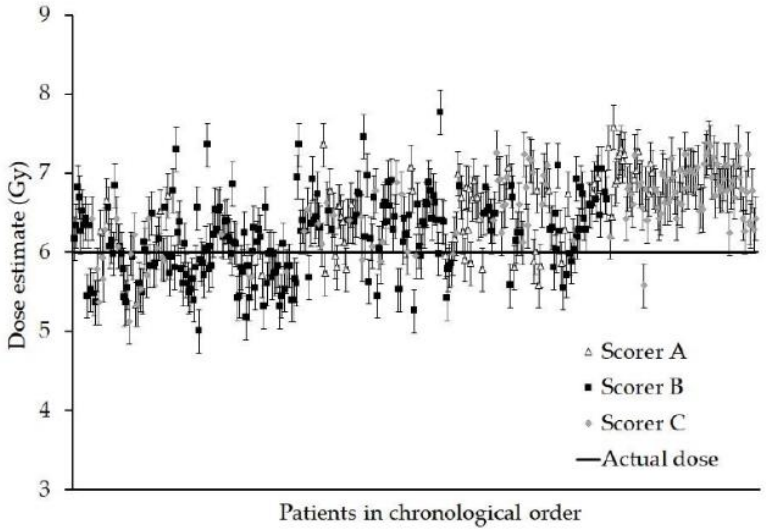

Fig. 20. The dose estimates and standard errors [58]

Dicentric chromosomes and other radiation dosimetric biomarkers have found uses outside of radiation protection and are used in therapeutic treatment. Cytogenetic assays can be useful techniques for personalized quantification of radiation effects in patients, providing relevant radiation dose estimates [59]. Cytogenetic assays are useful for comparison of different radiotherapy techniques and for dose estimation after mixed field exposures [60, 61].

With DC assay it is possible to estimate not only whole-body exposure but also partial-body exposure [27, 35]. This is very important, for example, for the analysis in radiotherapy patients [67]. "The cytogenetic indication of a partial body exposure is a non-Poisson distribution of dicentrics among the patient's scored metaphases" [27]. In other words, partial or whole-body exposure is determined by the distribution of aberrations: whether the aberrations are evenly distributed in the cells (whole-body exposure) or whether there are many healthy cells and a small number of cells with many aberrations (partial). Moreover, the distribution of dicentrics in cells differs depending on the areas of exposure, according to the results of various studies [62]. Hence, lymphocyte dispersion throughout the body is not uniform.

For a long time, various biodosimetry studies have included in vitro irradiation of the patient's blood samples and in vivo irradiation of a patient to simulate radiotherapy treatment and to compare physical and biological dose estimations. In the case of dicentric chromosomes and micronuclei, a previous study found a significant percent variance between the measured value (biological dosimetry) and the calculated value (physical dosimetry). One probable explanation is that the frequency of aberrations in cancer patients irradiated with the same dosage varies from person to

person. In the case of unstable aberration (dicentric chromosomes and micronuclei), the study found that inter-individual variance is much higher than in the case of stable aberration (translocations) [63].

DCA in peripheral blood lymphocytes from prostate cancer patients was used in one of studies to analyze the biological effect of the prolonged dose delivery time in modulated RT techniques, VMAT and IMRT, compared to conventional RT. The results revealed a statistically significant decrease of dicentric chromosomes after radiation using modulated techniques [64]. Comparisons of biological absorbed dose between different techniques are presented in Table 3 and Figure 21.

Table 3. Comparison of the median biological absorbed dose between the 3D-CRT, IMRT, and VMAT techniques [64]

Irradiation Technique	Median Value [min, max] (Gy)		Comparison	*p*-Value	
	Lymphocytes	PC3 Cells		Lymphocytes	PC3 Cells
3D-CRT	2.100 [1.988, 2.150]	2.070 [2.040, 2.130]	3D-CRT/IMRT	<0.05	<0.05
IMRT	1.980 [1.930, 2.050]	2.000 [1.980, 2.050]	IMRT/VMAT	0.3055	0.1270
VMAT	1.980 [1.900, 1.990]	1.970 [1.960, 2.010]	3D-CRT/VMAT	<0.05	<0.05

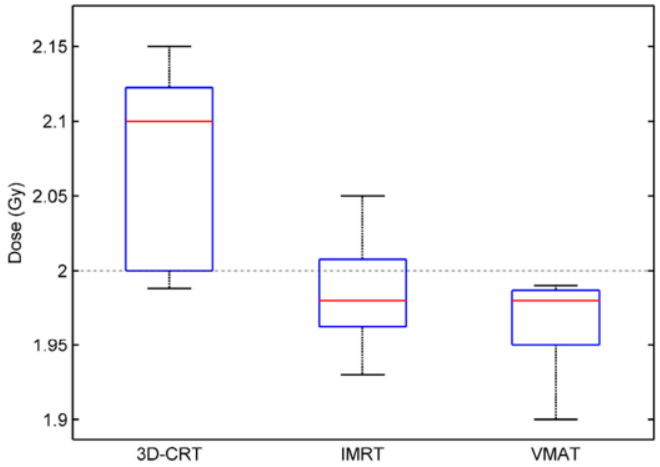

Fig. 21. Box and whisker plots of the biological absorbed dose across all prostate cancer patients [64]

Twelve patients with breast cancer who received identical radiation treatment (50 Gy in 25 fractions) were included in a recent study. Before, during, and after radiotherapy, lymphocytes were taken from patients to evaluate chromosome aberrations (dicentric chromosomes and translocations), which were then used to estimate whole-body and partial-body absorbed doses. They discovered a correlation between their biologically estimated whole-body doses and their physically calculated whole-body doses (Fig. 22). During radiation, the frequency of dicentric chromosomes increased in all patients [65].

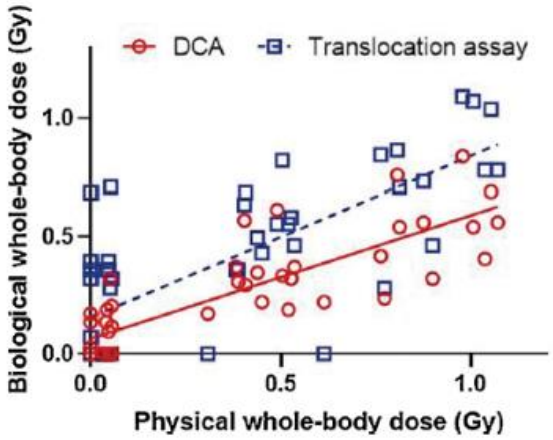

Fig. 22. Correlation between physically and biologically estimated whole-body radiation doses [65]

Biological dosimetry is also used for the comparison of external beam radiotherapy and brachytherapy. In one of the studies, the relationship between biodosimetric parameters and treatment volumes in prostate radiotherapy (low dose rate (LDR), high dose rate (HDR) brachytherapy and external beam radiotherapy (EBRT)) was analyzed [66]. From Figure 23 it can be seen that the highest amount of dicentrics and rings are in the case of EBRT.

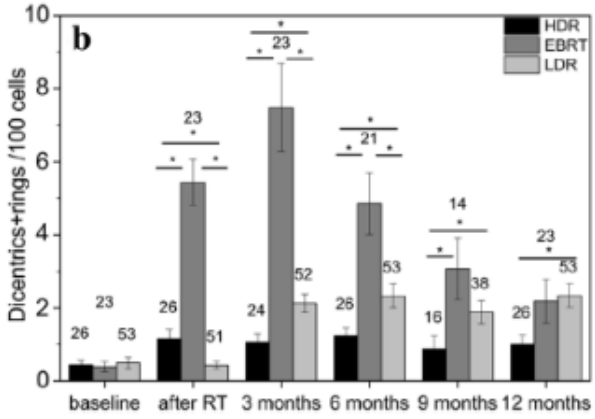

Fig. 23. Chromosome aberrations (dicentrics + rings) induced by three radiotherapeutic modalities [66]

As mentioned earlier, the dose can also be determined some time after the course of radiotherapy. One of the research evaluated the persistence of various types of aberrations up to 2.5 years following therapy. The yield of dicentrics was reduced to 40% of the initial value, whereas the quantity of translocations remained steady [68].

Summarizing the studies discussed above, it can be observed that DCA is also compared with other methods [69] and a more detailed analysis requires a complex evaluation of all biodosimetric assays.

It is important to note that ideally the radiation type of the in vitro dose response curve should coincide with the radiation being analyzed. However, previous studies have found that megavoltage LINAC X-rays have biological effects that are similar to ^{60}Co X-rays. The mean photon energy of 6 MV X-rays, for example, is 1.7 MeV, which is similar to the mean photon energy of ^{60}Co γ-rays, which is 1.25 MeV. In one of the investigations, in vitro dicentric dose response curves of 6 MV X-rays and ^{60}Co X-rays were created and compared. Except for a 13.8% higher β value for 6 MV X-rays, the

dose response curves of both radiation qualities were nearly identical. Blind testing, on the other hand, demonstrated that both of these curves are biologically similar and had a good dose accuracy rate [70].

1.7.2. Radiosensitivity

Depending on human radiosensitivity, ionizing radiation can cause different effects in the body. Therefore, an assessment of individual radiosensitivity could be used as an aid in optimizing radiation treatment.

Despite the fact that cytogenetics has been employed for a long time as a biomarker of radiation exposure, its application as an indicator of radiation sensitivity has been restricted. The findings of studies support the idea that cytogenetic analysis might be beneficial as a predictor of radiosensitivity.

The goal of one of the studies was to assess the in vitro lymphocyte response in prostate cancer patients in order to find potential radiosensitivity indicators. The sensitive individuals' blood samples showed a notable increase in dicentric chromosomes after 6 Gy when compared to the control group (Fig. 24) [71].

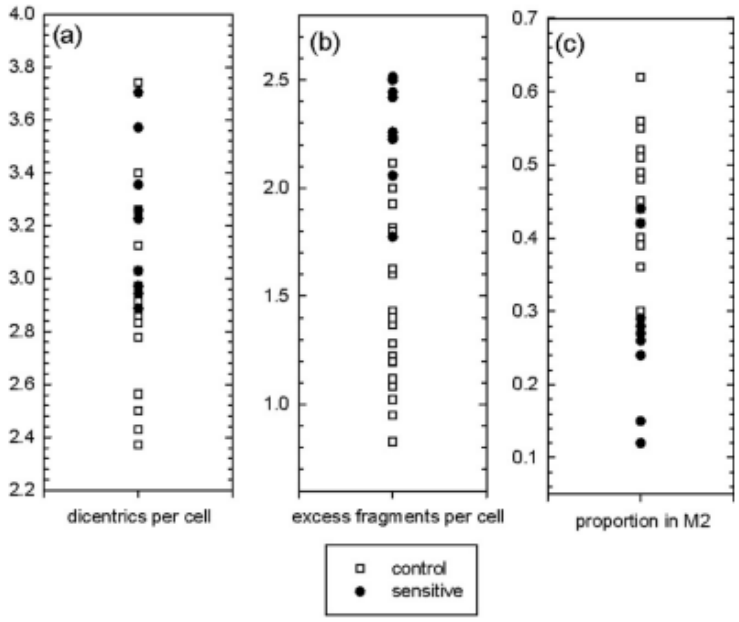

Fig. 24. Spread of the data for each of the endpoints: (a) dicentrics per cell, (b) excess fragments per cell, and (c) proportion of cells in M2. Each point represents 1 patient [71]

However, individual radiosensitivity is proposed to be assessed using the cytokinesis-block micronucleus and G2 chromosomal radiosensitivity assays. "The G2 chromosomal radiosensitivity assay or, simply G2 assay, measures the number of chromatid type aberrations induced by radiation in G2 phase." [72]

The result is expressed as a ratio of selected patient radiosensitivity and patient with Ataxia Telangiectasia (AT) radiosensitivity (2.5.1). Ataxia Telangectasia syndrome is a human syndrome characterized by mutations in the ATM protein that results in failure to repair DNA damage at the G2 stage of the cell cycle, thereby greatly increasing the risk of cancer. Assuming that people with this

syndrome are maximally sensitive to ionizing radiation by artificially simulating the presence of the syndrome in any human blood sample, one can compare a person's natural sensitivity to ionizing radiation with the maximum possible. Artificial simulation of AT is performed by adding caffeine to the blood lymphocyte culture, which removes the G2 checkpoint by caffeine at which the DNA repair takes place.

Lithuania's RPC began participating in the IAEA-coordinated research project "MEDBIODOSE: Applications of Biological Dosimetry Methods in Radiation Oncology, Nuclear Medicine, Diagnostic and Interventional Radiology" in 2017 to expand its work in the field of radiosensitivity. During the implementation of this project together with Klaipėda University Hospital and the National Cancer Institute, cytogenetic methods are used to investigate a possible link between the development of side effects caused by radiotherapy and radiosensitivity of people with cancer [73, 74].

In one of the studies of the Lithuania's RPC and other institutes micronuclei and G2 assays were compared for assessment of radiosensitivity [73]. The G2 assay was found to be more sensitive than micronuclei assay in this case.

The aim of another study was to analyze the effect of individual radiosensitivity on the development of side effects in prostate cancer patients [74]. Distribution of individual radiosensitivity in cancer patients during radiotherapy is presented in Figure 25. Individual radiosensitivity (IRS) calculated as a percentage of the high radiosensitivity level of patients with Ataxia-Telangiectasia (A-T) syndrome using equation IRS = (G2/G2 caffeine) × 100%. Interestingly, patients who had a rise in IRS during radiotherapy (RT) (patients No. 1, 5, and 6) and were radiosensitive or very radiosensitive at the end of RT also suffered RT-induced 1-2 grade acute GU/GI toxicity.

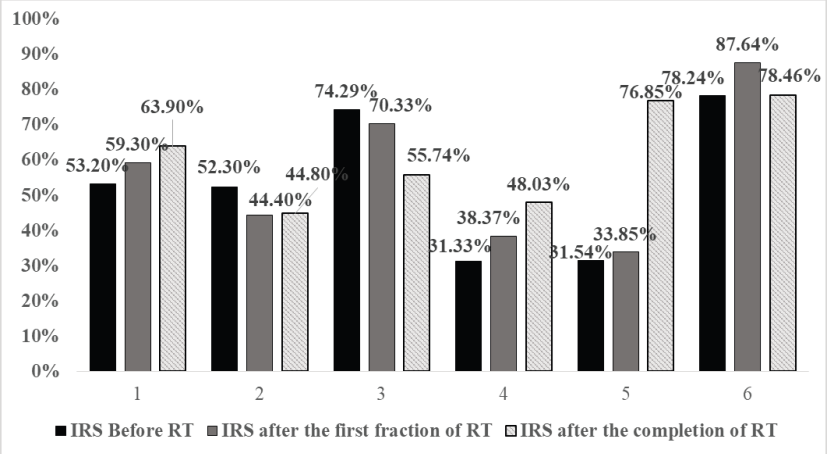

Fig. 25. Distribution of IRS in cancer patient in different phase of radiotherapy [74]

One of the latest studies of the Lithuania's National Cancer Institute and other institutes called: "Individual Radiosensitivity as a Risk Factor for the Radiation-Induced Acute Radiodermatitis" showed that the IRS determined before RT had no prognostic value for the development of Acute Radiodermatitis [75].

However, prediction of acute or late radiation toxicity can be done with cytogenetic markers, which is used for biodosimetry [76]. The review [77] summarized this kind of research. The average ex vivo induced yield of the cytogenetic markers was greater in patients with heavy responses than in individuals with a lower degree of normal tissue toxicity (NTT) in almost half of the relevant reports.

In summary, there is no consensus on the use of biomarkers, typically used for biodosimetry, in optimizing radiotherapy treatment or predicting side effects. This study was done to see if combination of DCA and individual radiosensitivity analysis can help to improve radiotherapy treatment and/or in predicting side effects that occur after radiotherapy and/or a radiological accident.

2. Materials and Methods

This section provides the materials and methods required to perform this study.

2.1. Irradiation of the Blood Samples and the Patients

For biological absorbed dose (DCA) and individual radiosensitivity (G2) analysis, six prostate cancer patients after prostatectomy, who were not previously exposed to ionizing radiation and had no genotoxic drugs treatment were chosen. The target for the radiotherapy (RT) plan was prostate/seminal vesicle bed and pelvic lymph nodes, and the organs at risk were bladder, small intestine, rectum, and femur heads. Patients were treated using volumetric modulated arc therapy (VMAT) technique using 6 MV photon beams (maximum dose rate of 600 MU/min). All patients received a total dose of 62–74 Gy, 2 Gy/day five times a week, which included dose to the pelvic lymphnodes 44–46 Gy, followed by a 16–28 Gy boost to the prostate/seminal vesicle bed (Table 4). Treatment planning was performed using program Eclipse 10.0.

Table 4. Information about the treatments

Patient	Dose delivered to pelvic lymphnodes (Gy)	Boost dose delivered to the prostate/seminal vesicle bed (Gy)	Total delivered dose (Gy)
1	46	28	74
3	46	20	66
4	46	16	62
5	44	28	72
6	46	16	62

The peripheral blood samples were taken three times 37etu p37h prostate cancer patient: prior to RT, after first fraction, and after completing RT. As an exception, blood sample of the sixth patient was taken three fractions earlier, after 62 Gy dose (total delivered treatment dose 66 Gy). It should be noted that the samples after the first fraction weren‘t analyzed.

The blood samples: prior to RT (2 Gy in vitro irradiation) and after completing RT (in vivo irradiation), were analyzed by the DCA to determine biological absorbed doses. 2 Gy in vitro 2 ml–4 ml blood samples irradiation was done with T-105 X-ray (Wolf Medizintechnik GmbH, Germany). Dose rate – 2.3 Gy/min and other parameters – 70 keV, 15 mA.

The blood samples: prior to RT and after RT, were analyzed by G2-assay to determine individual radiosensitivity (IRS) of patients.

2.2. Preparation of Cell Cultures

Blood cultures were 37etu p according to the protocol established at Lithuania‘s RPC which follows the IAEA recommendations [27] and the ISO standards [78, 79].

For the DCA and G2-assay: Peripheral blood was sampled to the Li-heparin vacutainers. Culturing of lymphocytes was done by adding 0.5 ml of heparinized whole blood to 4.5 ml of prepared mixture, that was done by adding 15 ml fetal bovine serum, 400 mM L-glutamine, antibiotics (1 ml

penicillin/streptomycin) and 2,4 ml (1 mg/ml) phytohaemagglutinin (PHA) to the 100 ml of F-10 medium (the specific amount of the mixture depends on the number of future cultures for which it is prepared). Incubation was done for 45 hours (for DCA) and 72 hours (for G2) in a humidified air atmosphere of 37°C in 5% CO_2.

For the DCA: After 45 hours, 150 µl of colcemid were added to each lymphocyte culture. The cultures were placed in the incubator for an additional 3 hours, leaving the same conditions.

For the G2-assay: After 72 hours lymphocytes cultures were in vitro irradiated to 1 Gy in T-105 X-ray therapy unit at room temperature (23 ± 2°C). Dose rate – 2.3 Gy/min (70 keV, 15 mA). After irradiation, the lymphocyte cultures were divided into two parts:

- 200 µl of caffeine solution (final mixture will be 4 mM) is added to one 5 ml lymphocyte culture tube.
- Caffeine was not added to the other part of the lymphocyte culture.

After splitting, the cultures were incubated at 37 ° C for 20 minutes. 150 µl of colcemid were added to each 5 ml culture tube to arrest at metaphase. The cultures were placed in the incubator for an additional 1 hour, leaving under the same conditions.

For the DCA and G2-assay: Centrifugation was used to collect peripheral lymphocytes, that were then resuspended in a 75 mM KCl solution for 15 minutes at 37 °C and rinsed three times in fixative (methanol – acetic acid, 3:1). The cell suspension was dropped with two 0.02 ml drops onto a microscope slide which has previously been slightly moistened with distilled water. The microscope slides were left to dry at room temperature. The painting mixture was prepared: 1 ml of Giemsa paint, 19 ml of double-distilled water. The slides were immersed in the staining vessel and kept for 3 minutes, then washed in water and left to dry.

2.3. Analysis with Microscope

Chromosome aberrations were analyzed with an Axio Imager Z2 microscope with a Metasystems Metafer slide analysis system. A CoolCube 1 digital camera was used to transfer the image to the computer. The image was displayed on a computer screen using Metafer 4.0 software and its plugins Msearch, AutoCapt.

The Msearch plug-in performed a metaphase-stage search on microscopic slides. Metaphase search was performed using a 10x lens with a sensitivity of 6.0 selected for the HorstTL classifier.

After that, 63x magnifying immersion lenses were attached and the AutoCapt plug-in was used to obtain more detailed images at higher magnifications.

Each image (cell) was examined, and a decision was made – whether the chromosomes are suitable for analysis, i. y. whether the image is bright enough or the chromosomes are not overlapped or twisted. Figure 26 shows the cell which is not suitable for DCA.

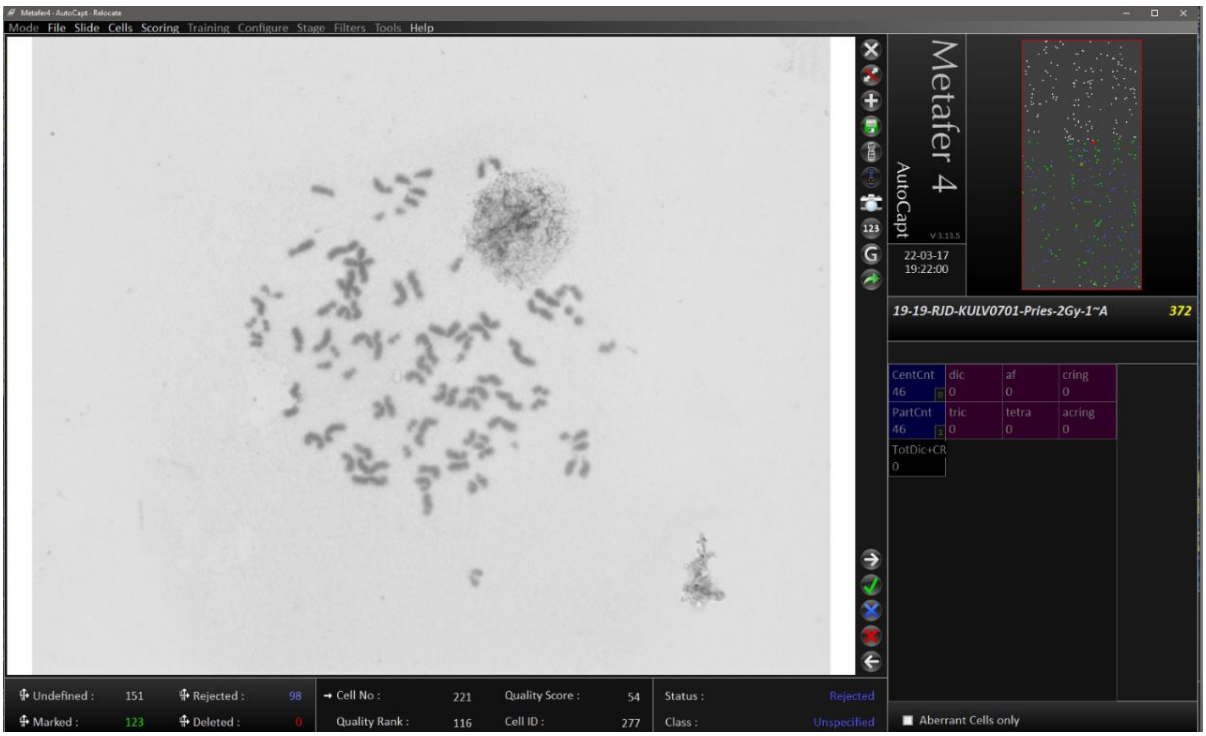

Fig. 26. Metasystems Metafer slide analysis software window. Cell image that is not suitable for analysis

After deciding to analyze the metaphase, the number of individual parts of the chromosomes were counted. Only complete sets of chromosomes were analyzed, i. y. sets of 46 or more individual parts of chromosomes and the number of centromeres must always be 46 ± 1.

2.4. Dicentric Chromosome Assay

When the set of chromosomes was found to be complete (as it is shown in Figure 27), the search for aberrations (dicentric chromosomes and ring chromosomes) was started.

Dicentric chromosomes were recorded with or without acentric fragments. The tricentric chromosome corresponds to two dicentrics, the quadricent chromosome to three dicentrics, and so on. Rings were also recorded with or without acentric fragments.

Fig. 27. Metasystems Metafer slide analysis software window. Cell image that is suitable for analysis

The analysis was completed by detecting 100 dicentric chromosomes per sample (patient). One sample can consist of several cultures. The results of the sample analysis are shown in Figure 28.

223 RSCdic/RSCdc_long Group X13- 2Gy in vitro

No	SlideName	ChngBy	ChngDate	ChngTime	NCells	Undefined	Rejected	Evaluated
1	7-17-RJD-X13-2Gy-1-2		22-02-27	14:55:27	111	1	59	51
2	7-17-RJD-X13-2Gy-3-2		22-03-09	13:12:55	152	0	80	72
3	7-17-RJD-X13-2Gy-4-4		22-03-06	17:39:57	43	0	17	26
4	7-17-RJD-X13-2Gy-4-5		22-03-06	19:15:39	41	0	20	21
5	7-17-RJD-X13-2Gy-1-4		22-03-09	12:54:39	93	8	57	28
6	7-17-RJD-X13-2Gy-2-1		22-03-09	11:19:45	18	1	13	4
7	7-17-RJD-X13-2Gy-2-2		22-03-09	12:38:57	48	0	27	21
7					506	10	273	223

Summary

dic	tric	tetra	cring	af	acring	TotDic+CR
101	0	0	1	139	0	102

Short Histogram (dicentrics + centric rings)

0 Ab.	1 Ab.	2 Ab.	3 Ab.	4 Ab.	>4 Ab.	>0 Ab.	total
135	75	12	1	0	0	88	223
60.5%	33.6%	5.4%	0.4%	0.0%	0.0%	39.5%	100.0%

No	Slide	CellNo	CellID	dic	tric	tetra	cring	af	acring	TotDic+C	CentCnt
2	1	3	15	1	0	0	0	1	0	1	47
3	1	4	55	1	0	0	0	3	0	1	45
4	1	5	57	1	0	0	0	2	0	1	44
5	1	8	127	1	0	0	0	1	0	1	46
6	1	9	138	0	0	0	0	1	0	0	45
7	1	16	178	2	0	0	0	3	0	2	44
8	1	17	184	1	0	0	0	2	0	1	44
9	1	19	186	1	0	0	0	5	0	1	44

Fig. 28. The results of the sample analysis

The absorbed dose was determined from the calibration dose-response curve (Fig. 29). This calibration curve is suitable for use to 5 Gy. The coefficients of the dose response curve for γ-rays (^{60}Co) were selected from those provided in the IAEA publication (Table 5) [27].

Table 5. The coefficients of the dose response curve [27]

C ± SE	α (Gy^{-1}) ± SE	B (Gy^{-2}) ± SE
0.00128 ± 0.00047	0.02103 ± 0.00516	0.06307 ± 0.00401

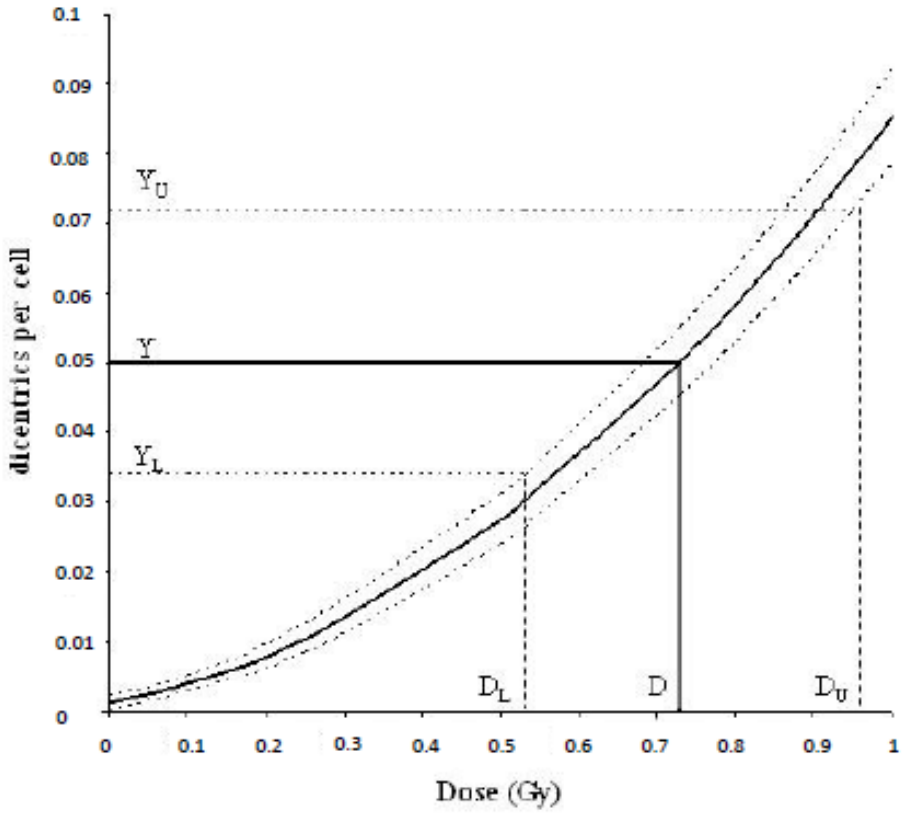

Fig. 29. A part of the dose–response calibration curve with its 95% confidence limits, used to estimate uncertainties [27]

The coefficients of the dose-response curve, the number of chromosomes analyzed and the number of dicentric and ring chromosomes found were entered into CABAS (Fig. 30), Dose Estimate (Fig. 31) and Biodose Tools (https://aldomann.shinyapps.io/biodosetools-v3/) (Fig. 32) [80] softwares.

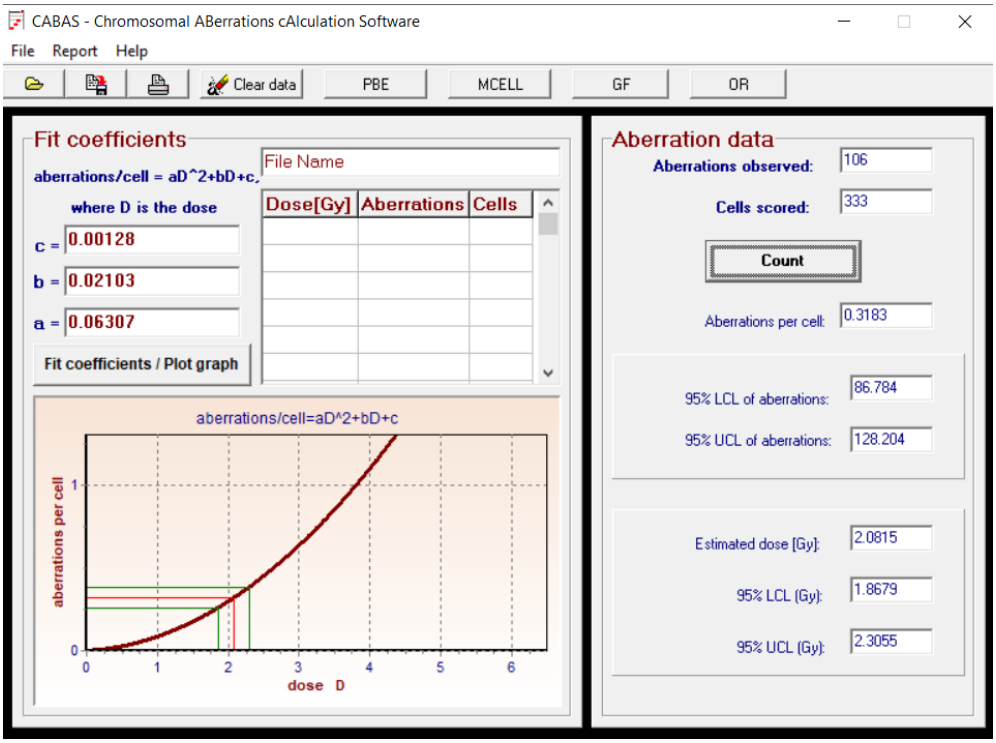

Fig. 30. CABAS software window

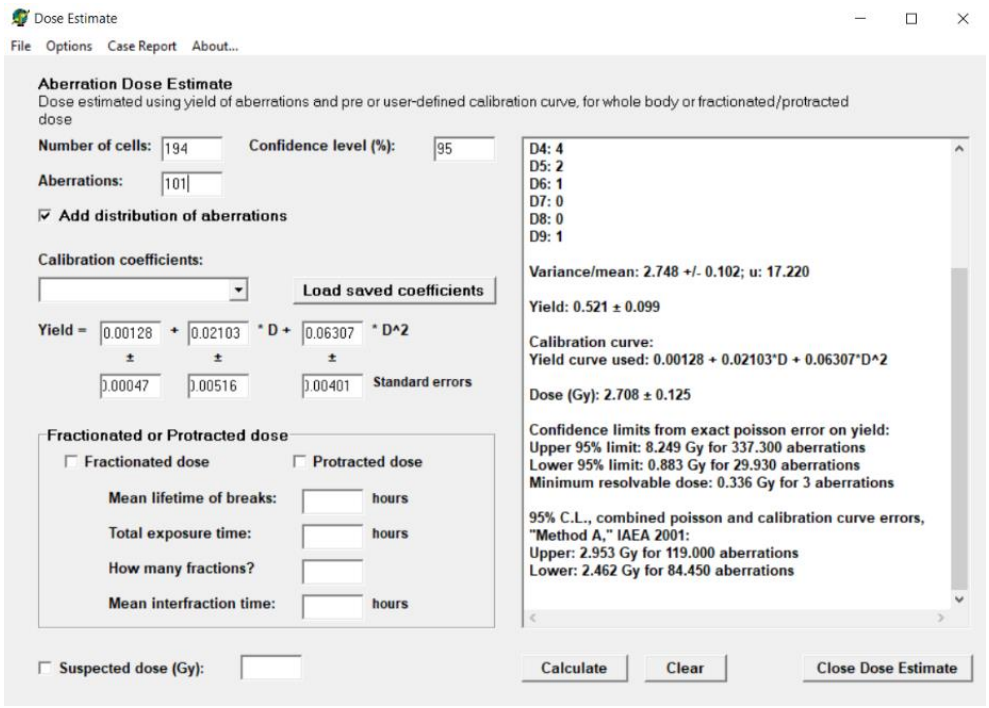

Fig. 31. Dose Estimate software window

Biodose Tools software is recognized for use in international research (for example RENEB).

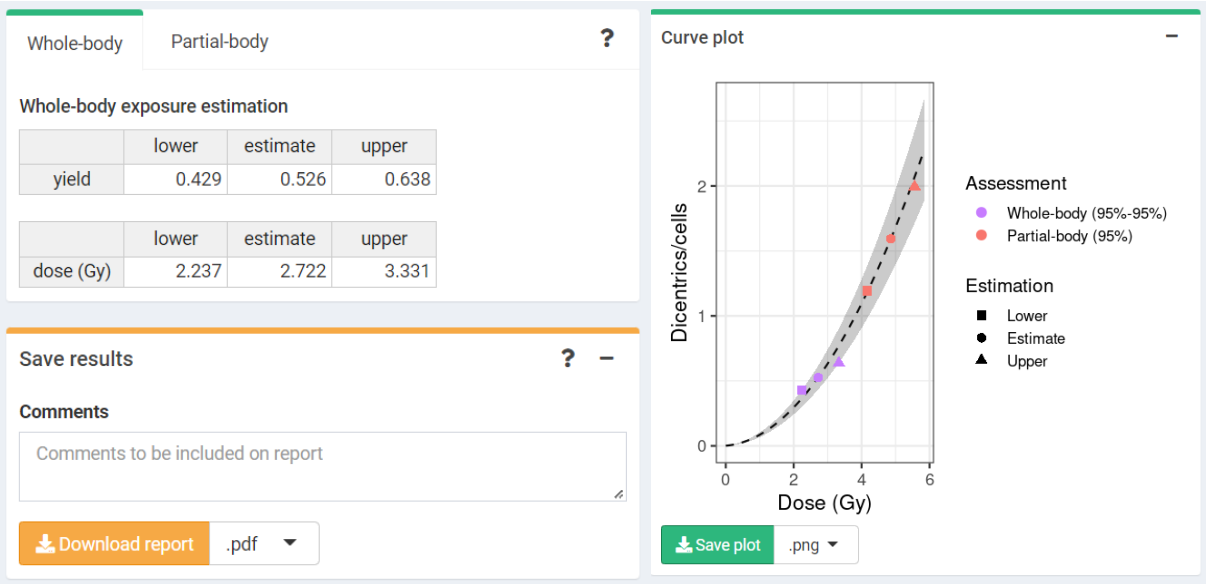

Fig. 32. Biodose Tool window

The softwares calculates the absorbed dose (Gy) and the upper and lower limits of 95% confidence and, if there was partial exposure, the percentage of body exposed.

2.5. G2-assay

When the set of chromosomes was found to be complete, chromosomes' and chromatids' breaks and gaps were analysed (Fig. 33).

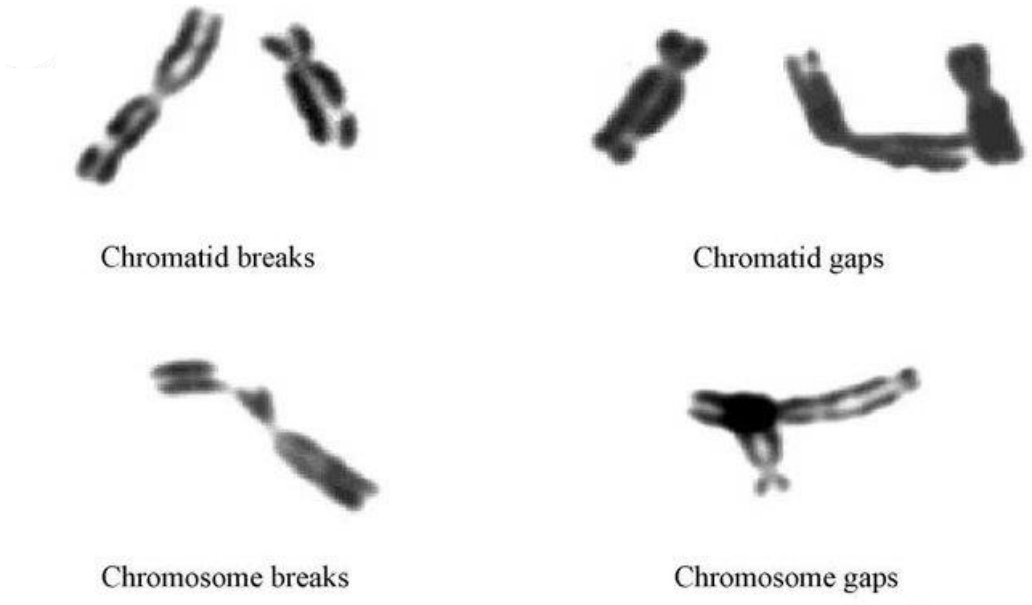

Fig. 33. Chromosomes' and chromatids' breaks and gaps [81]

To perform G2-assay, 50 metaphase-stage cells from a sample with caffeine and the same number of cells from a sample without caffeine were analyzed.

The individual radiosensitivity to ionizing radiation is determined according to the formula proposed by Pantelias at al. [82]:

$$IRS = \frac{G2}{G2_{caff}} \times 100\% \quad (2.5.1)$$

where IRS – individual radiosensitivity expressed as a percentage of the high radiosensitivity level of AT patients; G2 is the number of chromosomes' breaks in the decaffeinated sample; $G2_{caff}$ is the number of chromosomes' breaks in the sample with caffeine.

Patients were classified according to IRS value as:

- radioresistant (IRS < 30%);
- normal (30% ≤IRS ≤ 50%);
- radiosensitive (IRS > 50%);
- highly radiosensitive (IRS > 70%).

2.6. Analysis of the Results

Estimated absorbed doses using DCA were compared with physical dose of 2 Gy. T-test (R software) was performed to see if the difference between biological and physical doses is significant.

Estimated doses were compared between patients and with the individual radiosensitivity assay results to see if it affects the results of DCA.

After the treatment, patients' absorbed doses were evaluated and compared with total delivered doses and individual radiosensitivity.

Individual radiosensitivity of each patient was evaluated using a G2-assay.

3. Results and Discussion

This section covers all the results of the study and comparisons with the relevant research projects.

3.1. Dicentric Chromosome Assay before the Radiotherapy Treatment

First, absorbed doses in blood samples after irradiation of 2 Gy were evaluated using the DCA. The highest number of aberrations (dicentrics and rings) in one cell was observed in the blood sample of patient 1. The images of the cells with 4 and 6 dicentrics are presented in Figure 34. These results show partial exposure (u-value higher than 1.96), however it could be due to the low-quality irradiation.

From Table 6 it can be seen that in the samples of patients 2, 3, 4 the number of analyzed cultures is the highest, however cultures of these patients had only a few cells which were suitable for analysis.

Table 6. Results of DCA before the treatment

Patient	Cultures	Evaluated cells	Rejected cells	Dic.+rings	Dic.+rings/ cell	Distribution of dicentrics+rings							$\sigma^2/\bar{y}$	u
						0	1	2	3	4	5	6		
1	3	333	141	105+1	0.318	247	72	12	0	1	0	1	1.308	3.990
2	7	223	273	101+1	0.457	135	75	12	1				0.841	-1.689
3	8	231	393	100+5	0.455	150	59	20	2				1.045	0.487
4	8	314	292	100+4	0.331	228	69	16	1				1.038	0.471
5	2	250	341	100+7	0.428	169	60	16	5				1.156	1.750
6	2	280	222	101+3	0.371	192	72	16					0.940	-0.717

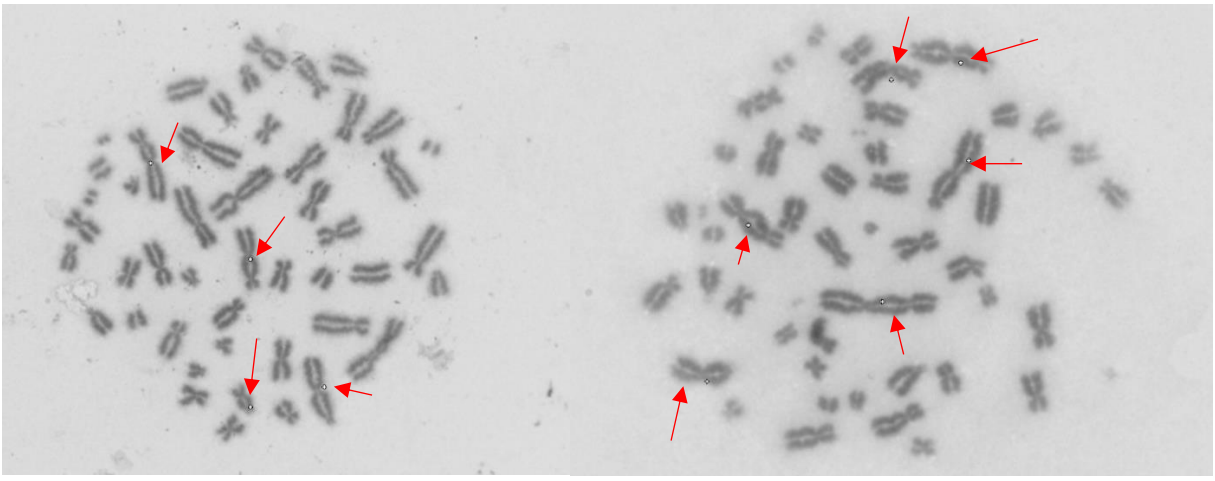

Fig. 34. The images of the cells with 4 and 6 dicentrics respectively

For the dose estimation different softwares – CABAS, Dose Estimate and Biodose Tool were used. Each program gives different uncertainty levels. IAEA presents three methods – A, B and C to estimate uncertainty. When the number of the detected aberrations is high, as it may be after high doses, Method A may be appropriate. When the uncertainty on the measured yield is similar to the uncertainty on the calibration curve, Approach B is generally the best option to use. The simplified method C considers the Poisson distribution in yield but ignores calibration curve errors. When the uncertainty on the measured yield surpasses the uncertainty on the calibration curve, which is

frequently the case at low doses, Approach C in its simplified form is acceptable [27]. For example, in the CABAS software confidence limits are from exact Poisson error on yield (Method C). Dose Estimate – combines Poisson and calibration curve errors (Method A). Biodose Tool – combines Poisson and calibration curve errors (Merkle method – B).

As all three programs give the same absorbed dose (Table 7), it was decided to use the Biodose Tool for further analysis, since it is acceptable for application in international research projects [49]

Table 7. Absorbed dose estimation results

Patient	**CABAS**			**Dose estimate**	**BiodoseTool**		
	Lower (Gy)	Estimate (Gy)	Upper (Gy)	Estimate ± uncertainty (Gy)	Lower (Gy)	Estimate (Gy)	Upper (Gy)
1	1.868	2.082	2.306	2.082 ± 0.109	1.702	2.081	2.555
2	2.267	2.528	2.802	2.528 ± 0.122	2.074	2.527	3.097
3	2.263	2.519	2.788	2.519 ± 0.121	2.070	2.519	3.082
4	1.907	2.127	2.357	2.127 ± 0.111	1.738	2.126	2.612
5	2.193	2.440	2.698	2.440 ± 0.118	2.005	2.439	2.984
6	2.029	2.262	2.506	2.262 ± 0.115	1.852	2.261	2.774

Comparison of estimated absorbed doses in each blood sample and delivered dose of 2 Gy is presented in Figure 35. It can be seen that absorbed doses are slightly overestimated. It should be noted that the absolute uncertainty of 0.5 Gy is acceptable in biological dosimetry [83].

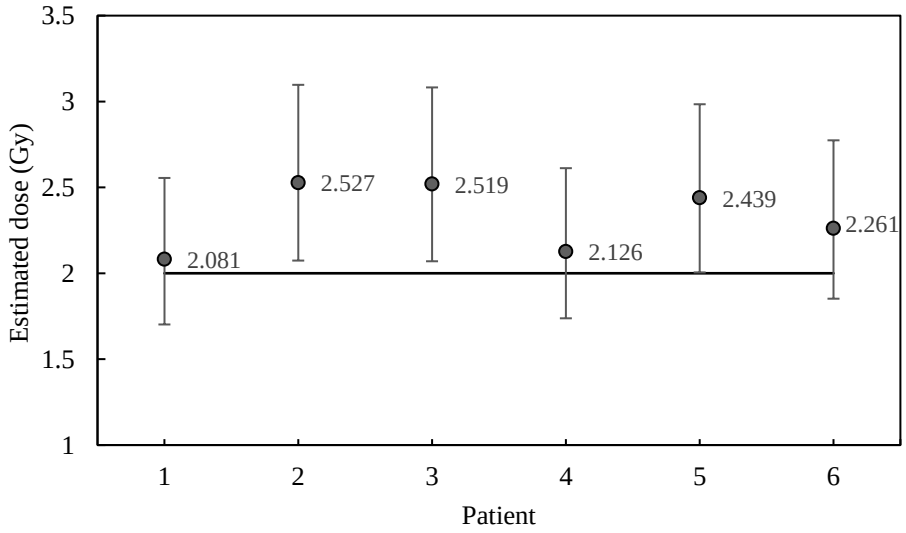

Fig. 35. Comparison of estimated absorbed doses in each patient sample and physical 2 Gy dose

The lowest relative uncertainties of estimated doses were observed in the samples of patient 1 and patient 4 (Fig. 36).

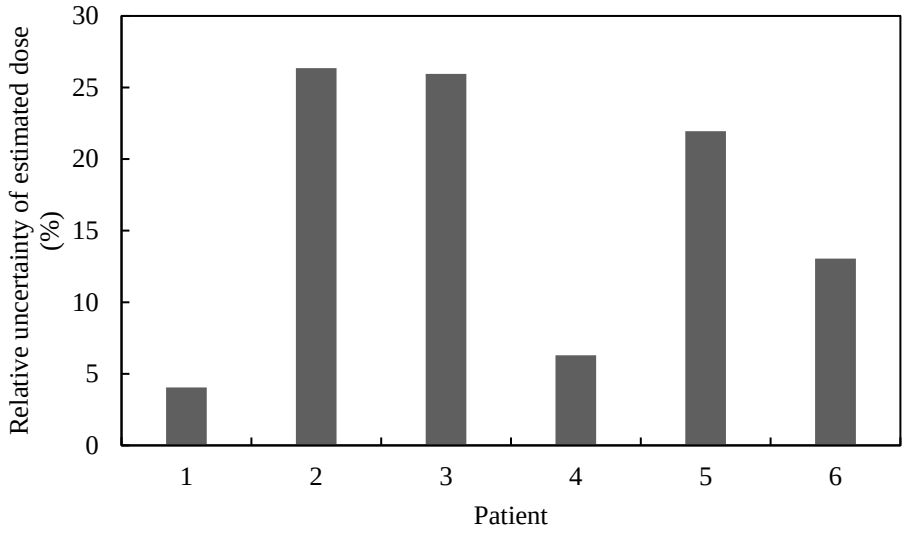

Fig. 36. Relative uncertainties of estimated doses comparison between the patients

From Figure 37 can be seen that it could be due to number of evaluated cells (the higher is the number of scored cells, the smallest relative uncertainty of estimated dose).

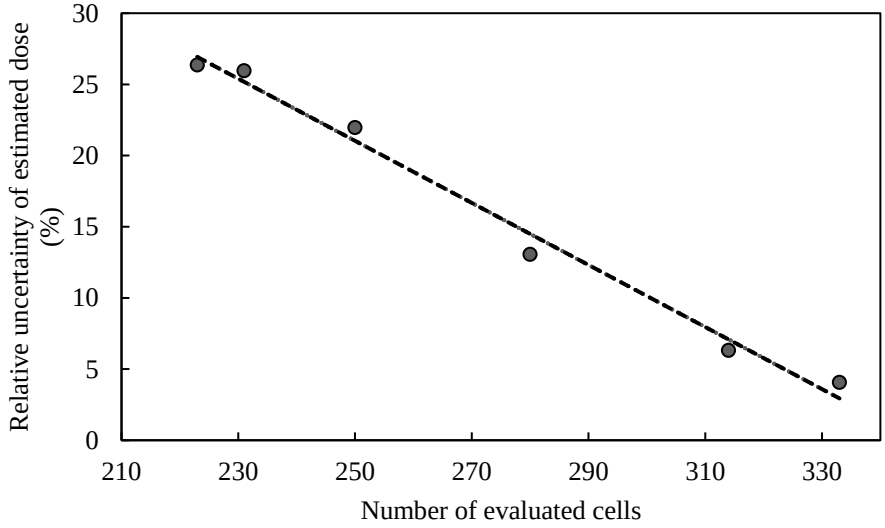

Fig. 37. Relative uncertainties of estimated doses comparison with number of evaluated cells

The t-test was performed to indicate whether the overestimation is statistically significant, because there is no minimum sample size required to do this test. Results showed that the mean of estimated doses (2.326) are significantly greater than delivered dose of 2 Gy (p-value 0.005) and the difference between this mean, and 2 Gy is statistically significant also (p-value 0.01). However, as it was mentioned before, the results with ±0.5 Gy uncertainty are acceptable.

Nikolakopoulou et al. [64] reported underestimated results in the case of in vitro irradiation with VMAT (Fig. 21). However, different irradiation conditions and another scorer can provide inverse results.

3.2. Dicentric Chromosome Assay after the Radiotherapy Treatment

After the RT treatment peripheral blood samples of each patient were analyzed by using DCA. Results are shown in Table 8. Distribution of dicentrics and rings is different than in the case of in vitro blood samples' irradiation of 2 Gy. After the treatment the maximum number of aberrations per cell was 10 and the minimum – 5, while after 2 Gy in vitro irradiation, the maximum number was 6 and the minimum number was 2. The image of the cell with 10 dicentrics is presented in Figure 38.

Unfortunately, culturing of lymphocytes for patient 2 was unsuccessful, so this patient was not analyzed after the treatment by DCA.

Table 8. Results of DCA after the treatment

Patient	Cultures	Evaluated cells	Rejected cells	Dic.+rings	Dic.+rings/cell	Distribution of dicentrics+rings											$\sigma^2/\bar{y}$	u
						0	1	2	3	4	5	6	7	8	9	10		
1	1	194	111	102+3	0.541	141	28	16	1	4	2	1	0	0	0	1	2.816	17.926
2	-	-	-	-	-												-	-
3	3	334	558	103+3	0.311	271	34	18	9	1	1						1.839	10.879
4	11	275	270	102+7	0.396	215	36	10	9	2	1	1	1				2.355	15.937
5	6	287	702	100+3	0.358	215	50	16	4	1	1						1.501	6.017
6	5	329	480	100+1	0.307	261	43	19	5	0	1						1.569	7.324

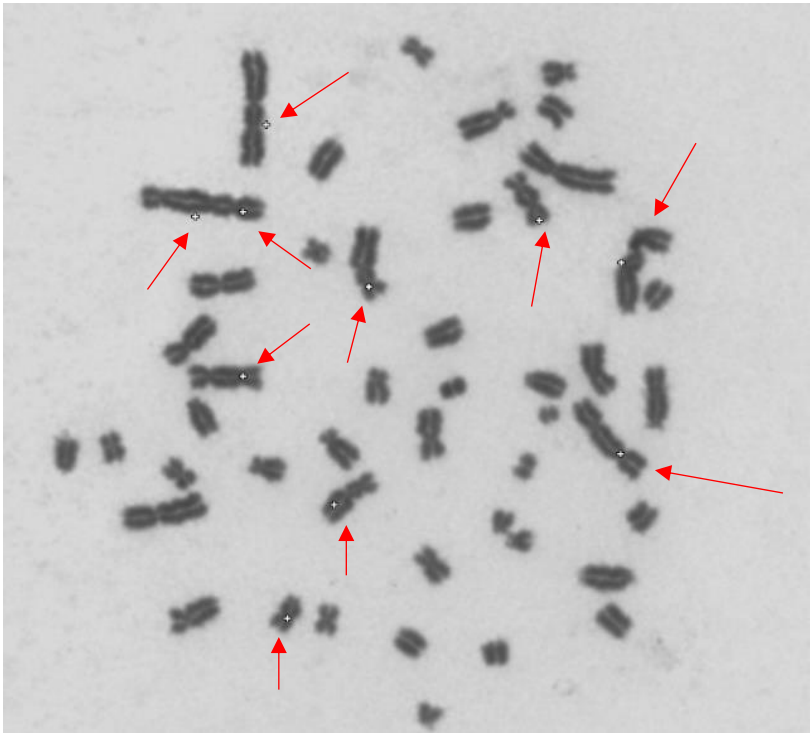

Fig. 38. The image of the cell with 10 dicentrics

Biodose Tool has the option to evaluate whole- and partial- body doses. However, only evaluation of whole-body doses makes a sense. Firstly, the volume of the body irradiated for prostate cancer patients is probably too small to get a reliable estimate of a partial-body dose. Secondly, the maximum

value of the dose-response curve used is 5 Gy and the applied doses were much higher. Finally, RT is a mixture of partial body exposure and fractionated exposure and there are no proper modes implemented in software for dose estimation in such cases. The suggestion to use a Biodose tool for partial-body dose estimations is based on the fact that one part of the body gets exactly an acute dose, and the other part of the body gets no dose at all. In our case, the same cells are not always exposed in each fraction. Some lymphocytes might get a relatively high dose (exposed during several fractions), some cells lower doses (exposed during few fractions only) and some cells are getting no dose at all. In other words: "In contrast to a single exposure, in which radiation is only applied to the cells in the irradiated field, a fractionated partial-body exposure distributes the radiation dose across a much larger portion of lymphocytes, due to migration of the cells following treatment." [65].

However, the evaluation of partial-body dose after the first fraction of RT will be important for the prediction of radiosensitivity of patients in future investigations. For the accurate results 1000 cells are needed for scoring.

The obtained results can be useful as a fact of evidence for radiation cell damage in partial-body exposure. Papworth's u-value shows the heterogeneity of irradiation. U-values which exceed ± 1.96 indicate that the distribution of aberrations deviated from a Poisson distribution and show non uniform exposure [65]. After the treatment the u-values range is 6.017–17.926, which indicates partial-body exposure. These results could be helpful, for example, for preparedness guidelines for nuclear accidents when personnel are partially exposed. Evidence of partial-body exposure can be observed more than 1 year after exposure [65, 68]. Dicentrics and translocations is one of the indicators for secondary cancers, so biological dosimetry analysis can provide information for individualized treatment after exposure.

Table 9. Results of absorbed dose estimation after the treatment

Patient	Total delivered dose (Gy)	Estimated whole-body dose (Gy)		
		lower	estimate	upper
1	74	2.276	**2.763**	3.377
3	66	1.699	2.078	2.551
4	62	1.925	**2.341**	2.864
5	72	1.816	2.220	2.726
6	62	1.663	2.041	2.513

Lee et al. [65] discovered a correlation between their biologically estimated and their physically calculated whole-body doses (Fig. 22). However, this work did not include physically calculated whole-body doses. From Figure 39 can be seen that the relationship between estimated whole-body doses and total doses delivered to patients during radiotherapy treatment was controversial, thus indicating that the results could be interpreted for each patient individually, since they could be affected by individual radiosensitivity. For example, for the patient 4 and patient 1, that had an increase in radiosensitivity during the radiotherapy treatment (Fig. 41), the estimated whole-body doses were the highest (Table 9).

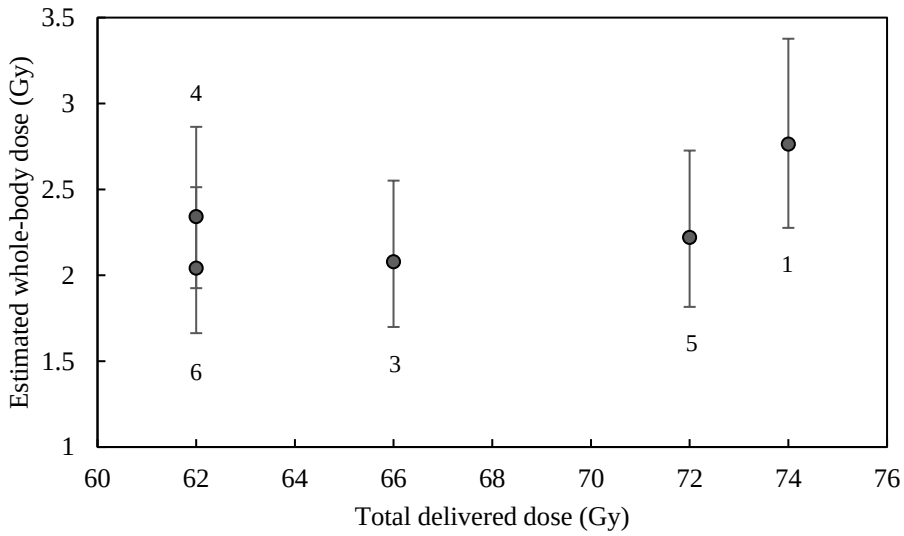

Fig. 39. Comparison of estimated whole-body doses and total doses delivered to patients (numbers indicate the patients)

3.3. Individual Radiosensitivity Analysis

After the DCA, individual radiosensitivity analysis using G2-assay was performed. The images of chromosomes with marked and not marked breaks and gaps are presented in Figure 40.

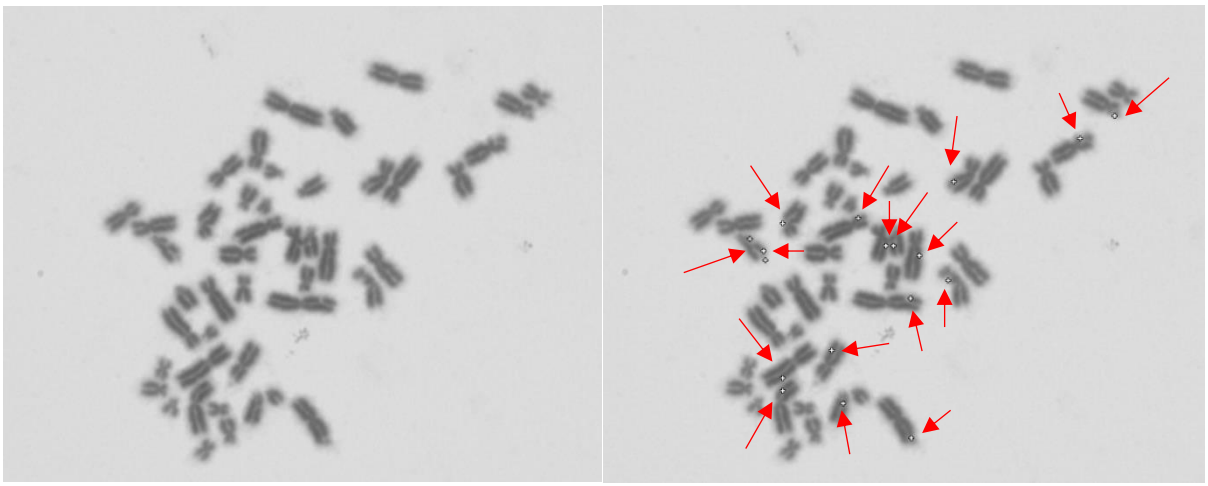

Fig. 40. The view of chromosomes. Left – chromosomes' and chromatids' breaks and gaps are not marked, right – marked

Obtained results are presented in Table 10. Most patients were evaluated as being highly radiosensitive, but the results might be influenced by the lack of experience of scorers and poor view of cells. In this situation relative results can be considered reliable. Patients were classified according to IRS value: patient 1 (before the treatment) – **normal**, patient 1 (after the treatment), patient 4 (before the treatment) and patient 5 (after the treatment) – **radiosensitive**, and all others – **highly radiosensitive**.

Table 10. Results of the individual radiosensitivity analysis

Patient	Before the treatment			After the treatment		
	No. of aberrations without coff.	No. of aberrations with coff.	IRS, %	No. of aberrations without coff.	No. of aberrations with coff.	IRS, %
1	230	517	44.49	331	474	69.83
2	420	566	74.21	-	-	-
3	451	580	77.76	499	636	78.46
4	502	716	70.11	430	458	93.89
5	585	619	94.51	368	656	56.1
6	478	586	81.57	349	456	76.54

Figure 41 shows the individual radiosensitivity of patients. It was found that for patient 1 and patient 4 individual radiosensitivity was increased after radiotherapy treatment, for patient 3 – slightly increased and for patients 5 and patient 6 – decreased. These results show that patient's sensitivity is a very individual issue. Ionizing radiation (especially low doses) can cause organism sensitization or adaptation [74], but every prediction of the sensitivity changes is very complicated.

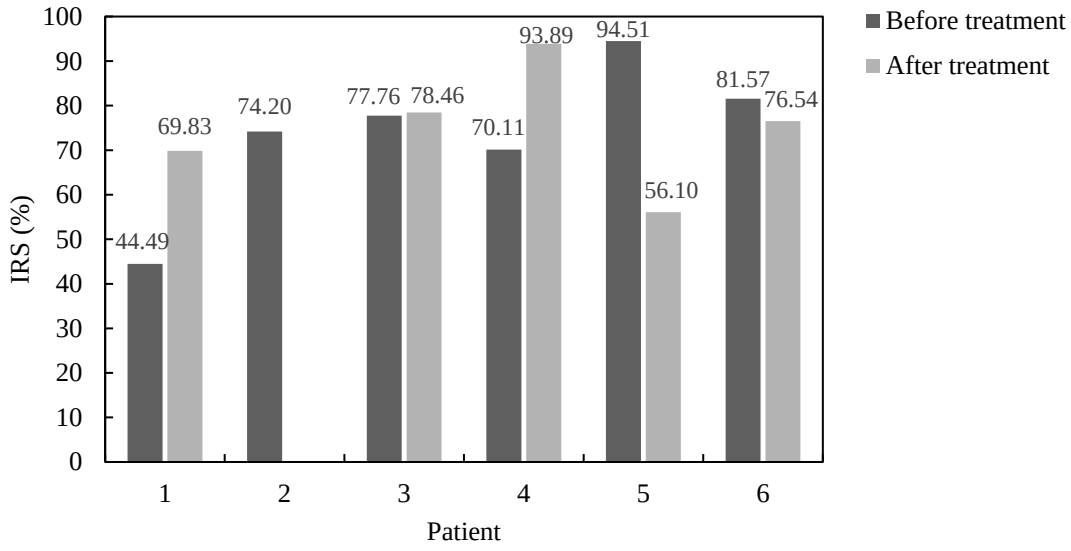

Fig. 41. Individual radiosensitivity of patients

One of the goals of IRS analysis was to identify whether the IRS affects the results of DCA analysis. Some correlation (Table 11 and Figure 42) between estimated dose and IRS before the treatment was found, but was not observed for all patients. Beaton et al. [71] reported DCA results showing that higher frequency of dicentrics aberrations after 6 Gy exposure were found for radiosensitive patients as compared to the control group. (Fig. 24). Thus, higher doses may be required to see a clearer correlation.

Table 11. Individual radiosensitivity and estimated absorbed dose before the treatment

Patient	IRS before treatment (%)	Estimated dose (2 Gy in vitro) (Gy)
1	44.48	2.081
2	74.20	2.527
3	77.76	2.519
4	70.11	2.126
5	94.51	2.439
6	81.57	2.261

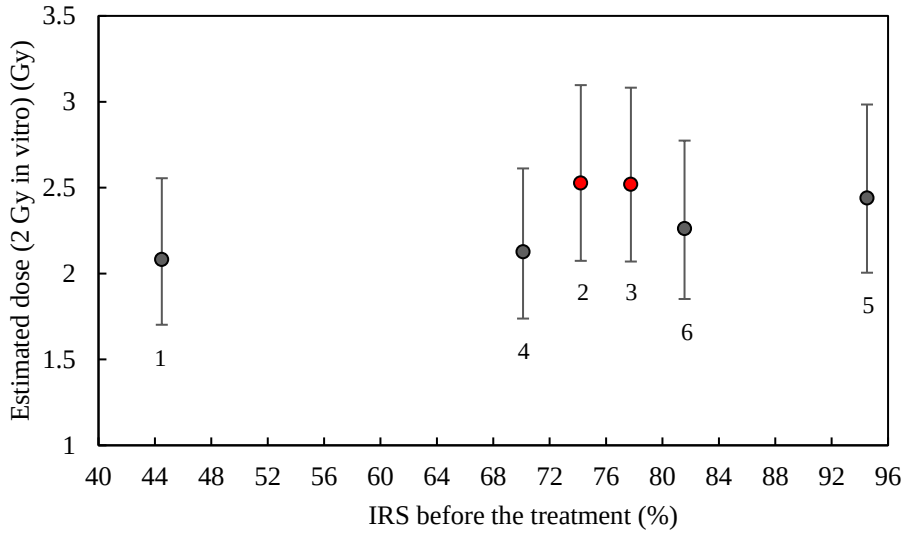

Fig. 42. Comparison of estimated absorbed dose and individual radiosensitivity before the treatment (numbers indicate the patients)

From Table 12 it can be seen that if the individual radiosensitivity tends to increase after treatment (patients 1 and 4) then the relative uncertainty of the estimated dose is low. If the individual radiosensitivity tends to decrease (patients 5 and 6) – relative uncertainty is higher. Except for the third patient (assessed by other scorer), where the change in the individual radiosensitivity during RT treatment is negligible.

It can be concluded that if the relative uncertainty of the estimated dose (2 Gy in vitro) is high and the patient is radiosensitivity prior to RT treatment, the IRS may will tend to decrease over the course of RT, with the result of fewer side effects, as it is described in Sevriukova et al. [74] research. Thus, the IRS assay prior to RT treatment alone may not indicate whether a patient will experience side effects. However, involved DCA after in vitro irradiation may help predict IRS change and the risk of side effects. With this information, RT can be individualized, however this requires more investigations.

Table 12. Comparison of individual radiosensitivity and estimated dose

Patient	IRS before treatment (%)	IRS after treatment (%)	Estimated dose (2 Gy in vitro) (Gy)	Relative uncertainty of estimated dose	Difference between IRS after and before treatment
1	44.48	69.83	2.081	**4.05**	**25.35**
2	74.2	-	2.527	26.35	-
3	77.76	78.46	2.519	25.95	0.7
4	70.11	93.89	2.126	**6.3**	**23.78**
5	94.51	56.1	2.439	21.95	-38.41
6	81.57	76.54	2.261	13.05	-5.03

From Table 13 and Figure 43 it can be seen that there is no correlation between estimated whole-body dose and IRS after the treatment.

Table 13. Individual radiosensitivity and estimated absorbed dose after the treatment

Patient	IRS after treatment (%)	Total delivered dose (Gy)	Estimated whole-body dose (Gy)
1	69.83	74	2.763
3	78.46	66	2.078
4	93.89	62	2.341
5	56.10	72	2.220
6	76.54	62	2.041

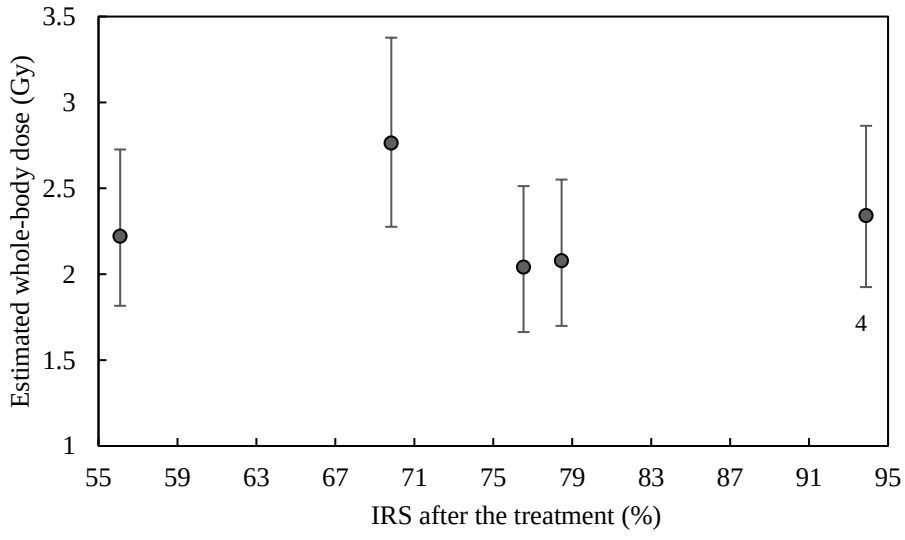

Fig. 43. Comparison of estimated whole-body absorbed dose and individual radiosensitivity before the treatment (numbers indicate the patients)

However, it should be noted that the total delivered doses are different for each patient, and it affects the results.

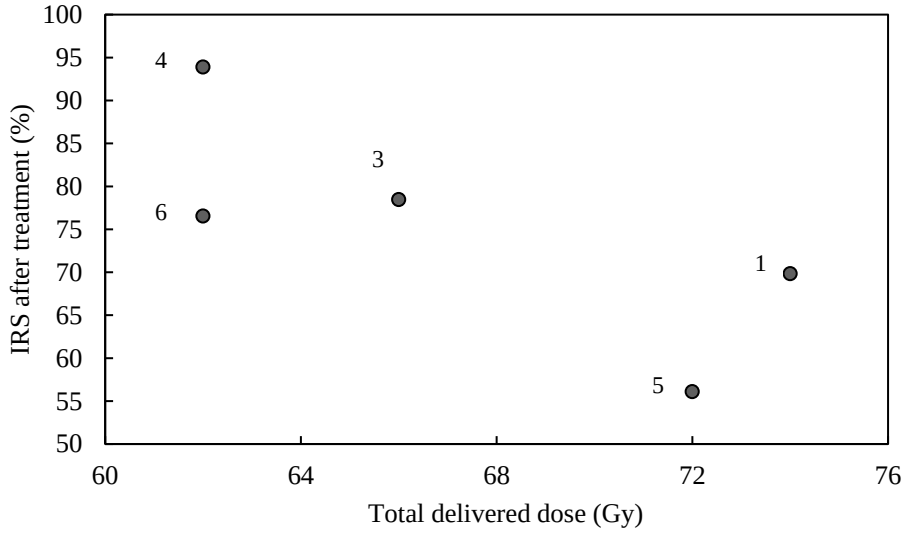

Fig. 44. Relationship between individual radiosensitivity and total delivered dose (numbers indicate the patients)

Figure 44 shows that if total delivered dose to the patient is lower (62 and 66 Gy) – patients are more radiosensitive (76.54–93.89%) and when total delivered dose is higher (72 and 74 Gy) – patients are less radiosensitive (56.10–69.83%). However, lower delivered doses cannot be considered to radiosensitize patients because changes in radiosensitivity during RT are individual (Fig. 41).

The correlation between the estimated dose before the RT treatment and the IRS is not clear (Fig. 42), but a correlation is possible after the RT treatment. This was particularly shown in the increase in radiosensitivity of patient 1 and patient 4 during RT treatment (Fig. 41) and the higher whole-body dose of these patients (Table 9). This coincides with the results of other authors [71, 76, 77]. Imano et al. [76] showed that the number of chromosome aberrations was higher in the overreactors group than in the non-overreactors group. In the Vinnikov et al. [77] review it is shown that almost half of the relevant reports indicate similar results like Imano et al.. However, not all of them proved the correlation between IRS and frequency of dicentrics and therefore further investigations are needed.

Conclusions

1. The comparison of estimated and delivered dose of 2 Gy has shown slight overestimation (2.082–2.528 Gy). The mean of estimated doses (2.326 Gy) was significantly higher than 2 Gy (p-value 0.005). However, it was acceptable since dose deviations up to 0.5 Gy are allowed according to recommendations. The lowest relative uncertainties of estimated doses were observed in the blood samples of patient 1 and patient 4, where numbers of scored cells were the highest. These results show that the Dicentric Chromosome Assay can be used for the accurate determination the absorbed doses of the blood samples.
2. Estimated whole-body doses after radiotherapy treatment were from the range of 2.041–2.763 Gy. Estimated Papworth's u-value ranged between 6.017–17.926, indicating partial-body exposure. These findings might be useful in developing preparedness guidelines for radiological incidents in which workers are partially exposed. The relationship between estimated whole-body doses and total doses delivered to patients during radiotherapy treatment was controversial, thus indicating that the results could be interpreted for each patient individually, since they could be affected by individual radiosensitivity.
3. Radiosensitivity analysis results showed that for patient 1 and patient 4 – individual radiosensitivity was increased, for patient 3 – slightly increased and for patient 5 and patient 6 – decreased. Therefore, patient can become either more or less radiosensitive during radiotherapy treatment. Clear correlation between estimated doses and individual radiosensitivity before and after radiotherapy treatment was not found. However, the increase in radiosensitivity of patient 1 and patient 4 patients during the radiotherapy course could be related to higher whole-body doses.
4. Combination of individual radiosensitivity and Dicentric Chromosome Assays may help to predict radiosensitivity changes, leading to individualized radiotherapy treatment, however more investigations are needed.

Acknowledgment

I wish to express my gratitude to the employees of Radiation Protection Centre, especially to dr. Olga Sevriukova who trained and advised me during the study.

I would also like to confer my thanks to medical physicist Aurimas Krauleidis and dr. Aista Plieskiene, head of Radiation Therapy Department of Klaipeda University Hospital, for the patients' blood samples and required information about the radiotherapy treatments.

Finally, I would like to thank prof. dr. Diana Adliene for her contribution in helping to prepare this thesis.

List of References

1. POŠKUS, Andrius. *Atomo fizika ir branduolio fizikos eksperimentiniai metodai*. Vilnius: Vilniaus universiteto leidykla, 2008. ISBN 9789955332954.
2. OSIBOTE, Otolorin Adelaja. Introductory Chapter: Radiation Exposure, Dose and Protection. *Ionizing and Non-ionizing Radiation*, 2020, 3.
3. United States Nuclear Regulatory Commision. *Measuring Radiation* [online]. 2017 [viewed 10 April 2022]. Access via: https://www.nrc.gov/about-nrc/radiation/health-effects/measuring-radiation.html
4. Korea Institute of Radiological and Medical Sciences. *Dose assessment* [online]. [viewed 10 April 2022]. Access via: https://www.kirams.re.kr/eng/nremc/activities04.jsp
5. ADLIENĖ, Diana and Gediminas ADLYS. *Spinduliuotės detektoriai*. Kaunas: Technologija, 2011. ISBN 9789955259282.
6. SHULTIS, J. Kenneth, Richard E FAW. *Fundamentals of Nuclear Science and Engineering Third Edition*. CRC press, 2016. ISBN 9781498769297.
7. CHAIKH, Abdulhamid, Arnaud GAUDU, Jacques BALOSSO. Monitoring methods for skin dose in interventional radiology. *International Journal of Cancer Therapy and Oncology*, 2014, 3.1: 03011.
8. Nuclear Power. *Active Dosimeters – Passive Dosimeters* [online]. [viewed 11 April 2022]. Access via: https://www.nuclear-power.net/nuclear-engineering/radiation-dosimetry/radiation-dosimeter/active-dosimeters-passive-dosimeters/
9. WILLIAMS, M. and P. METCALFE. Radiochromic film dosimetry and its applications in radiotherapy. *In AIP Conference Proceedings*, vol. 1345, 75–99, AIP, 2011.
10. PODGORSAK, Ervin B., et al. *Radiation oncology physics*. Vienna: IAEA, 2005.
11. ROSENBLATT, Eduardo, et al. Relevance of particle therapy to developing countries. *International Journal of Radiation Oncology, Biology, Physics*, 2016, 95.1: 25-29.
12. LEDINGHAM, Ken WD, et al. Towards laser driven hadron cancer radiotherapy: A review of progress. *Applied Sciences*, 2014, 4.3: 402-443.
13. MOHAMAD, Osama, et al. Carbon ion radiotherapy: a review of clinical experiences and preclinical research, with an emphasis on DNA damage/repair. *Cancers*, 2017, 9.6: 66.
14. HADA, Megumi, et al. Association of inter-and intrachromosomal exchanges with the distribution of low-and high-LET radiation-induced breaks in chromosomes. *Radiation research*, 2011, 176.1: 25-37.
15. American Cancer Society. *Getting External Beam Radiation Therapy* [online]. [viewed 14 April 2022]. Access via: https://www.cancer.org/treatment/treatments-and-side-effects/treatment-types/radiation/external-beam-radiation-therapy.html
16. DELGADO, A. Brito, et al. Modeling the target dose fall-off in IMRT and VMAT planning techniques for cervical SBRT. *Medical Dosimetry*, 2018, 43.1: 1-10.
17. MOHAN, Gomathi, et al. Recent advances in radiotherapy and its associated side effects in cancer—a review. *The Journal of Basic and Applied Zoology*, 2019, 80.1: 1-10.
18. MOLLAH, Abdus Sattrar. PLUNC 3D Radiation Treatment Planning System (TPS): An Educational Platform for Medical Physics Students. *Bangladesh Journal of Nuclear Medicine*, 2018, 21.1: 35-42.
19. WAMBERSIE, A., et al. Prescribing, recording, and reporting photon beam therapy presentation of the ICRU report# 50. *Journal of Medical Physics*, 1992, 17.4: 5.

20. Įveik vėžį. *Prostatos vėžys* [online]. 2020 [viewed 20 April 2022]. Access via: https://www.iveikvezi.lt/prostatos-vezys/
21. Mayo Clinic. *Prostate* [online]. [viewed 20 April 2022]. Access via: https://www.mayoclinic.org/diseases-conditions/prostate-cancer/symptoms-causes/syc-20353087
22. Urologas Kaune. *Prostatos vėžys, rizikos veiksniai* [online]. 2017 [viewed 20 April 2022]. Access via: https://www.urologaskaune.lt/prostatos-vezys-rizikos-veiksniai/
23. WHO. Globocan 2020. *Prostate cancer in Lithuania* [online]. 2020 [viewed 20 April 2022]. Access via: https://gco.iarc.fr/today/data/factsheets/populations/440-lithuania-fact-sheets.pdf
24. Prostate cancer UK. *Treatments. External beam radiotherapy* [online]. [viewed 22 April 2022]. Access via: https://prostatecanceruk.org/prostate-information/treatments/external-beam-radiotherapy
25. DANCE, D. R., et al. *Diagnostic radiology physics: A handbook for teachers and students*, 2014.
26. JOINER, Michael C. and Albert J. VAN DER KOGEL. *Basic clinical radiobiology*. CRC press, 2018.
27. AINSBURY, E., et al. *Cytogenetic dosimetry: applications in preparedness for and response to radiation emergencies*, 2011.
28. BfS. *Hereditary radiation damage* [online]. [viewed 25 April 2022]. Access via: https://www.bfs.de/EN/topics/ion/effect/hereditary/hereditary_node.html
29. HABER, Alan H. and Barbara E. ROTHSTEIN. Radiosensitivity and rate of cell division: "Law of Bergonie and Tribondeau". *Science*, 1969, 163.3873: 1338-1339.
30. The University of Waikato Te Whare Wananga o Waikato. *DNA, chromosomes and cells.* Access via: https://www.sciencelearn.org.nz/images/198-dna-chromosomes-and-cells
31. GOODHEAD, Dudley T. Initial events in the cellular effects of ionizing radiations: clustered damage in DNA. *International journal of radiation biology*, 1994, 65.1: 7-17.
32. MIRREZAEI, Ehsan, et al. Construction and validation of in vitro dose–response calibration curve using dicentric chromosome aberration. *Radiation Protection Dosimetry*, 2020, 189.2: 198-204.
33. AINSBURY, E. A., et al. Review of retrospective dosimetry techniques for external ionising radiation exposures. *Radiation protection dosimetry*, 2011, 147.4: 573-592.
34. WOJCIK, Andrzej, et al. The RENEB operational basis: complement of established biodosimetric assays. *International journal of radiation biology*, 2017, 93.1: 15-19.
35. SHIRLEY, Ben C., et al. Estimating partial-body ionizing radiation exposure by automated cytogenetic biodosimetry. *International Journal of Radiation Biology*, 2020, 96.11: 1492-1503.
36. SUTO, Yumiko, et al. Cytogenetic examination of human peripheral blood lymphocytes cryopreserved after gamma irradiation: A pilot study. *Cytologia*, 2020, 85.1: 71-77.
37. HAGMAR, Lars, et al. Cancer risk in humans predicted by increased levels of chromosomal aberrations in lymphocytes: Nordic study group on the health risk of chromosome damage. *Cancer research*, 1994, 54.11: 2919-2922.
38. ROSSNER, Pavel, et al. Chromosomal aberrations in lymphocytes of healthy subjects and risk of cancer. *Environmental health perspectives*, 2005, 113.5: 517-520.
39. FUCIC, Aleksandra, et al. Frequency of acentric fragments are associated with cancer risk in subjects exposed to ionizing radiation. *Anticancer research*, 2016, 36.5: 2451-2457.
40. REMM. *About Dicentric Chromosome Assays*. Access via: https://remm.hhs.gov/aboutdicentrics.htm

41. BALAJEE, Adayabalam S. Applications of fluorescence in situ hybridization in radiation cytogenetic biodosimetry and population monitoring, 2018.
42. PRASANNA, Pataje GS, Maria MORONI, Terry C. PELLMAR. Triage dose assessment for partial-body exposure: dicentric analysis. *Health physics*, 2010, 98.2: 244.
43. PYATKIN, E. K., V. Yu NUGIS, A. A. CHIRKOV. Absorbed dose estimation according to the results of cytogenetic investigations of lymphocyte cultures of persons who suffered in the accident at the Chernobyl Atomic Power Station. *Meditsinskaya Radiologiya* (USSR), 1989, 34.6.
44. HAYATA, Isamu, et al. Cytogenetical dose estimation for 3 severely exposed patients in the JCO criticality accident in Tokai-mura. *Journal of radiation research*, 2001, 42. SUPPL: S149-S155.
45. KUBOTA, Yoshihisa, et al. Chromosomal aberrations in wild mice captured in areas differentially contaminated by the Fukushima Dai-Ichi Nuclear Power Plant accident. *Environmental science & technology*, 2015, 49.16: 10074-10083.
46. INTERNATIONAL ORGANIZATION FOR STANDARDIZATION (ISO). Radiation protection–Performance criteria for service laboratories performing biological dosimetry by cytogenetics. Geneva: ISO, 2004, 19238: 2014.
47. INTERNATIONAL ORGANIZATION FOR STANDARDIZATION (ISO). Radiation protection–Performance criteria for laboratories performing cytogenetic triage for assessment of mass casualties in radiological or nuclear emergencies–General principles and application to dicentric assay. *General principles and application to dicentric assay*. Geneva: ISO, 2008, 21243: 2008.
48. RENEB [online]. [viewed 1 May 2022]. Access via: https://www.reneb.net/
49. ENDESFELDER, David, et al. RENEB/EURADOS field exercise 2019: robust dose estimation under outdoor conditions based on the dicentric chromosome assay. *International Journal of Radiation Biology*, 2021, 97.9: 1181-1198.
50. WOJCIK, Andrzej, et al. The RENEB operational basis: complement of established biodosimetric assays. *International journal of radiation biology*, 2017, 93.1: 15-19.
51. PORT Matthias, Ursula OESTREICHER, David ENDESFELDER and Michael ABEND. RENEB biological and physical dosimetry study laboratory inter-comparison of eight dosimetry assays.
52. IAEA. Response and Assistance Network (RANET) [online]. [viewed 1 May 2022]. Access via: https://www.iaea.org/services/networks/ranet
53. WILKINS, R. C., Z. CARR, D. C. LLOYD. An update of the WHO Biodosenet: Developments since its Inception. *Radiation protection dosimetry*, 2016, 172.1-3: 47-57.
54. GUOGYTĖ, Kamilė, et al. Dicentrinių chromosomų analizės metodo taikymas nustatant apšvitą. *Visuomenės sveikata*, 2016.
55. THIERENS H., et al. Cytogenetic biodosimetry of an accidental exposure of a radiological worker using multiple assays. *Radiation Protection Dosimetry*, 2005; 113(4):408-414.
56. LI, Yanxin, et al. Automated discrimination of dicentric and monocentric chromosomes by machine learning-based image processing. *Microscopy research and technique*, 2016, 79.5: 393-402.
57. SHEN, Xiang, et al. A dicentric chromosome identification method based on clustering and watershed algorithm. *Scientific Reports*, 2019, 9.1: 1-11.
58. MOQUET, Jayne, et al. Radiation biomarkers in large scale human health effects studies. *Journal of Personalized Medicine*, 2020, 10.4: 155.

59. VINNIKOV, Volodymyr, Oleg BELYAKOV. Clinical Applications of Biological Dosimetry in Patients Exposed to Low Dose Radiation Due to Radiological, Imaging or Nuclear Medicine Procedures. *Seminars in Nuclear Medicine*. WB Saunders, 2021.
60. WOOLF, David K., et al. Biological dosimetry for breast cancer radiotherapy: a comparison of external beam and intraoperative radiotherapy. *Springerplus*, 2014, 3.1: 1-6.
61. BASTIANI, Isabella, et al. Dose estimation after a mixed field exposure: Radium-223 and intensity modulated radiotherapy. *Nuclear Medicine and Biology*, 2022, 106: 10-20.
62. SREEDEVI, B., et al. Chromosome aberration analysis in radiotherapy patients and simulated partial body exposures: biological dosimetry for non-uniform exposures. Radiation protection dosimetry, 2001, 94.4: 317-322.
63. VENKATACHALAM, P., et al. Estimation of dose in cancer patients treated with fractionated radiotherapy using translocation, dicentrics and micronuclei frequency in peripheral blood lymphocytes. *Mutation Research/Fundamental and Molecular Mechanisms of Mutagenesis*, 1999, 429.1: 1-12.
64. NIKOLAKOPOULOU, Aggeliki, et al. Comparison and Evaluation of Different Radiotherapy Techniques Using Biodosimetry Based on Cytogenetics. Cancers, 2022, 14.1: 146.
65. LEE, Younghyun, et al. Chromosome aberration dynamics in breast cancer patients treated with radiotherapy: Implications for radiation biodosimetry. *Mutation Research/Genetic Toxicology and Environmental Mutagenesis*, 2021, 872: 503419.
66. KOCSIS, Zsuzsa S., et al. Relationship between biodosimetric parameters and treatment volumes in three types of prostate radiotherapy. *Scientific reports*, 2021, 11.1: 1-10.
67. MOQUET, Jayne, et al. Dicentric dose estimates for patients undergoing radiotherapy in the RTGene study to assess blood dosimetric models and the new Bayesian method for gradient exposure. *Radiation research*, 2018, 190.6: 596-604.
68. HARTEL, Carola, et al. Persistence of radiation-induced aberrations in patients after radiotherapy with C-ions and IMRT. Clinical and translational radiation oncology, 2018, 13: 57-63.
69. MANIVANNAN, Bhavani, et al. A comparison of estimates of doses to radiotherapy patients obtained with the dicentric chromosome analysis and the γ-H2AX assay: Relevance to radiation triage. Applied Radiation and Isotopes, 2018, 131: 1-7.
70. KUMAR, A. Arul Anantha, et al. Comparison of dicentric dose response curves of 6 MV LINAC X-rays and 60Co γ-rays for biodosimetry application. *Applied Radiation and Isotopes*, 2017, 129: 124-129.
71. BEATON, Lindsay A., et al. Chromosome damage and cell proliferation rates in in vitro irradiated whole blood as markers of late radiation toxicity after radiation therapy to the prostate. *International Journal of Radiation Oncology* Biology* Physics*, 2013, 85.5: 1346-1352.
72. HASKINS, Jeremy S., Takamitsu A. KATO. G2 chromosomal radiosensitivity assay for testing individual radiation sensitivity. *Radiation Cytogenetics*. Humana, New York, NY, 2019. p. 39-45.
73. GUOGYTĖ, Kamilė, et al. Micronuclei and G2 assays for assessment of chromosomal radiosensitivity as assistant tool in radiotherapy: method-comparison study. *Sveik. Moksl.*, 2016, 26: 63-68.
74. SEVRIUKOVA, Olga, et al. Effect of radiotherapy-induced alteration of individual radiosensitivity on development of side effect in cancer patients. *Health Sci*. East. Eur, 2020, 30: 48-52.
75. KIŠONAS, Juras, et al. Individual Radiosensitivity as a Risk Factor for the Radiation-Induced Acute Radiodermatitis. *Life*, 2021, 12.1: 20.

76. IMANO, Nobuki, et al. Evaluating Individual Radiosensitivity for the Prediction of Acute Toxicities of Chemoradiotherapy in Esophageal Cancer Patients. *Radiation Research*, 2021, 195.3: 244-252.
77. VINNIKOV, Volodymyr, et al. Prediction of the acute or late radiation toxicity effects in radiotherapy patients using ex vivo induced biodosimetric markers: A review. *Journal of Personalized Medicine*, 2020, 10.4: 285.
78. INTERNATIONAL ORGANIZATION FOR STANDARDIZATION (ISO). Radiation protection–Performance criteria for laboratories performing cytogenetic triage for assessment of mass casualties in radiological or nuclear emergencies–General principles and application to dicentric assay. General principles and application to dicentric assay. Geneva: ISO, 2008, 21243: 2008.
79. INTERNATIONAL ORGANIZATION FOR STANDARDIZATION (ISO). Radiation protection–Performance criteria for service laboratories performing biological dosimetry by cytogenetics. Geneva: ISO, 2004, 19238: 2014.
80. HERNÁNDEZ, A., et al. Biodose Tools: An R Shiny Application for Biological Dosimetry [online]. 2020 [viewed 10 May 2022]. Access via: https://biodosetools-team.github.io/biodosetools/
81. PAZ-Y-MIÑO, César, et al. Should gaps be included in chromosomal aberration analysis?: evidence based on the comet assay. *Mutation Research/Genetic Toxicology and Environmental Mutagenesis*, 2002, 516.1-2: 57-61.
82. PANTELIAS, Gabriel E. and Georgia I. TERZOUDI. A standardized G2-assay for the prediction of individual radiosensitivity. *Radiotherapy and Oncology*, 2011, 101.1: 28-34.
83. LLOYD, D. C., et al. The role of cytogenetics in early triage of radiation casualties. *Applied Radiation and Isotopes*, 2000, 52.5: 1107-1112.